POLITECNICO
DI TORINO

School of Engineering

Politecnico di Torino

Master Thesis

Design of a model-based control for a bulge test

Prepared by

Ali Al Ali

Univ.-Prof. Dr.-Ing. Luigi Mazza

M.Sc. M.Sc. Gunnar Matthiesen

The present work was submitted to

Institute for Fluid Power Drives and Systems
RWTH Aachen University

Univ.-Prof. Dr.-Ing. Katharina Schmitz

Master Thesis

Design of a model-based control for a bulge test

Submitted by:	*Cand. Master. Ali Al Ali*
Politecnico Supervisor:	*Prof. Luigi Mazza*
IFAS Supervisor:	*M.Sc. M.Sc. Gunnar Matthiesen*
Field of activity:	*Pneumatic, Control Design*

Aachen, March 2019

DEDICATION

I want to dedicate this work for my professor Univ.-Prof. Dr.-Ing. Luigi Mazza, Univ.-Prof. Dr.-Ing. Katharina Schmitz and M.Sc. M.Sc. Gunnar Matthiesen for their help, advice, and support during my work on this thesis. In addition, I dedicate my project for my family, Yasmine and my friends who stay with me and give me advice push up and support.

From my heart thank you all, your support helps me to success.

Table of contents

I Formula symbols

i	Current	[A]
V	Voltage	[V]
l	Length of the solenoid	[m]
N	Number of turn	[-]
Φ	Magnetic flux	[Wb]
B	Magnetic flux density	[Wb/m^2]
A	Area of the coil	[m^2]
H	Magnetic field strength	[A/m]
μ	Permeability	[H/m]
μ_0	Permeability of free space	[H/m]
μ_r	relative magnetic permeability	[-]
Pb	hysteresis loss	[w]
Pe	eddy current loss	[w]
P_{fe}	Residual loss	[w]
B_{max}	maximum flux density	[Wb/m^2]
f	frequency of magnetic reversals per second	[Hz]
η	Steinmetz hysteresis coefficient, depending on material	[J/m^3]
t_0	material thickness	[m]
V	volume of magnetic material	[m^3]
K_e	eddy current constant	[-]
n	constants depending on material	[-]
m	constants depending on material	[-]
R	Resistance	[Ω]

λ	Flux linkage	[Wb-t]
x	Position of the plunger	[m]
$\dot{x}$	Velocity of the plunger	[m/s]
$E_{(x,i)}$	Over all co-energy	[N/m]
F_{tot}	Total force on the plunger	[N]
F_{hooke}	Spring force	[N]
F_w	Armature weight	[N]
F_μ	Friction	[N]
F_{vis}	Viscosity force	[N]
k_4	Sum of Armature weight and Viscosity force	[N]
M	Mass of the plunger	[Kg]
β	Viscosity	[Kg/m·s]
K	Spring constant	[-]
θ	Force angle	[°]
Ld	Dynamic inductance	[H]
Ls	Static inductance	[H]
Wm	Magnetic field energy	[N/m]
e	Inductive electromotive force	[V]
B_0	Initial magnetic flux density	[Wb/m^2]
H_0	Initial magnetic field strength initial	[A/m]
ΔH	magnetic field strength	[A/m]
ΔB	the variations of magnetic flux density after applying a current disturbance	[Wb/m^2]
Br	the valve iron core flux density	[Wb/m^2]
r	Effective sectional area of the magnetic flux within the valve core	[m]
H_m	Magnetic field strength of magnetic material	[A/m]

H_g	Magnetic field strength of the air gap	[A/m]
l_m	length of the magnetic material	[m]
l_g	length of the air gap	[m]
ε	Strain level	[-]
$\dot{\varepsilon}$	strain rate	[-]
P	pressure	[pa]
$\sigma_{1,2}$	Stresses along the principal-stress	[N/m^2]
$\rho_{1.2}$	The curvature radius	[m]

II Abbreviations

IFAS	Institute for Fluid Power Drivers and Systems
HGBT	Hot Gas Bulge Test
SSV	State space variable
SMO	Sliding mode observer
SMC	Sliding mode control
VSS	variable structure system
SISO	single input single output

1 Introduction

Electromagnets and solenoid valves are wide-spread actuators in industrial and other applications, due to their robustness, rather simple design, relatively high force density (force per unit mass) and relatively low cost. In particular, fast switching valve have a relatively large force to weight ratio and high speed characteristics thus they have been useful in actuation for pneumatic and hydraulic systems, and are applied e.g in Pressure control valves for Hot Gas Bulge Test (HGBT), internal combustion engines as gas exchange valves, fuel injection valves, or antilock braking system (ABS) valves.

However, a simple and cheap design of solenoids often makes the actuators exhibit a highly nonlinear dynamics, which makes them difficult to control or even to use as self-sensing actuators. Enhanced control design and self-sensing strategies try to enable the use of cheap and simple constructed solenoids in the aforementioned sophisticated fields. Furthermore, apart from cost reasons, it is often not possible to apply position sensors, e.g. due to insufficient space or unfavourable environment. Especially for solenoid actuators with small air-gap it is difficult to realize a sufficiently accurate position measurement in mass production. It is therefore necessary to have a better control of the motion and force of this solenoid valve.

In this study an advanced nonlinear model for a fast switching solenoid will be developed. In which, to circumvent implementation of additional sensor, research in the area of sensorless position estimation based on quantities that can be easily measured, such as voltage and current, is ongoing since several years. For that goal, the Solenoid model is designed based on the mechanical and electrical characteristic of the valve, and using experimental data, which related to its electromagnetic characteristic of the valve, to estimate the plunger movement in real time.

With a simple ON–OFF switching-valve control, early studies focused on optimizing the valve electromagnetic-pneumatic/hydraulic characteristics to improve

the pressure modulation. Nowadays, many more sophisticated control methods were adopted for such test, which needs a real-time controller to achieve precise linear control for the applied flow rate. For that reason, knowing the position of the plunger inside the valve is needed. Thus, there is an urgent need for a new technology to improve the control of low-cost high-speed switching valve, making its performance comparable to that of proportional valves, thus obtaining more accurate linear pressure characteristic with little noise. To solve this problem, linear control of high-speed switching valve has been proposed to be a promising method. Earlier research has showed that the proportional solenoid valve can be controlled with pulse width modulation (PWM) of the coil supply voltage. As for the switching valve, despite the strong nonlinearity in the electromagnetic characteristics, accurate position control of the valve plunger can also be performed by advanced model control based on estimated parameter which derived experimentally, to perform the valve model and get the plunger movement with time.

With the necessary computational power at hand, sophisticated algorithms are used to estimate the movement in real time, even in low cost applications. Observer state estimation appear attractive, as such algorithms may be simple in their realization, and exhibit strong robustness toward bounded disturbances and parameter variations. It takes the solenoid model as a reference, and it can achieve fast error convergence with an appropriate correction factor, i.e. observer injections gains.

An attractive method in designing the model based position estimator is by the Sliding Mode (SM) estimation technique, due to its robustness to uncertainties, speed of convergence and nonlinear structure. This involves obtaining a model of the system with its available measurements. The estimator is a copy of the system model, with its input being the system input and the mismatch between the measured output and the estimated output, namely the error. The mismatch is passed through a discontinuous function of the error and then multiplied by a feedback gain. This is then added to the observer equations, the intension being that the estimation error of all the unmeasured states could be reduced to some neighbourhood

of zero in finite time. Hence, the unmeasured states could be reconstructed from the available measurements and the system input.

This thesis is organized as follow. Initially, background information about fluid power system, the electromagnetism of the solenoid valve, and the type of solenoid valve. Then two different methods for designing the solenoid valve model are introduced with brief theoretical information about the observer, and then about the Bulge test which is the purpose of using the valve application in this experiment. Third part consists of two points, the technical information about the valve used in the test bench, then a brief explanation about the experimental control system used to find the electromagnetic force exerted by the solenoid. The Forth Part presents the required measurements with their simulation, and the used setup for each measurement. The Fifth Part presents the setup used to design the Sliding mode observer, its structure and the model used to find the missing parameter. The Sixth Part presents the validation of the observer performance using Matlab Simulink. Finally the summary of the project is presented with outlooks about future research.

2 Theoretical Background

This chapter presents the general idea of fluid power system, its type, structure and property. Then the solenoid valve is presented as a device used to control or regulate the flow of the fluid power system, in which the solenoid electromagnetism and material property are presented in the second part. In the third part the solenoid valve types and two modelling methods that can be used to design the valve model are presented. In the fifth part a brief theoretical information about the observer types and property are presented, taking into account the sliding mode observer one. Finally a brief explanation about the Bulge test bench, for which the solenoid and the observer model are designed, is presented.

2.1 Fluid power system

Fluid power is a term describing hydraulics and pneumatics technologies. Both technologies use a fluid to transmit power from one location to another. With hydraulics, the fluid is a liquid (usually oil), whereas pneumatics uses a gas (usually compressed air). Both are forms of power transmission, which is the technology of converting power to a more useable form and distributing it to where it is needed, such system commonly known as fluid power systems.

The basic structure of fluid power system is consisting of pumps (compressor) which convert the mechanical energy into hydraulic or pneumatic energy, conduits (storage, filter, heat exchanger, filter, pipes) to transfer the fluid power, and the motoric section (linear motor, rotating motor, and valves) which uses it to create a linear or rotating motion. It easily produces linear motion using hydraulic or pneumatic cylinders and can transmit equivalent power within a much smaller space compared to electric driver technologies, especially when extremely high force or torque is required. It offers simple and effective control of direction, speed, force, and torque using simple control valves.

Pneumatic systems have many properties that make them attractive for use in a variety of environments. They are less sensitive to temperature than hydraulic systems and offer many advantages for positioning applications. Low maintenance cost, cleanliness and safety are some of these advantages. However, they are suffering from common drawbacks including friction and sensitivity of actuator dynamics to load and piston position along the cylinder stroke. In addition, from a control perspective, controlling a pneumatic actuator is a challenge because the system dynamics are non-linear. The non-linear nature of a pneumatics system exacerbated when it uses on/off solenoid valves, which have widespread applications due to the high cost of servo valves [NFP17].

A valve is a device that regulates, directs or controls the flow of a fluid by opening, closing, or partially obstructing various passageways. Figure 2-1 shows the Schematic of simple solenoid valve. The main component of this valve is the orifice (1), plunger (2), coil (3) and the return spring (4). However, the valve components are different according to their function and type. Valves actuated by different ways, which are pneumatic, mechanical, and electromechanical actuation, and this choice mostly based on the application purpose, the intended degree of automation, the kind of signal processing in the control, the size of the valve and the safety regulation.

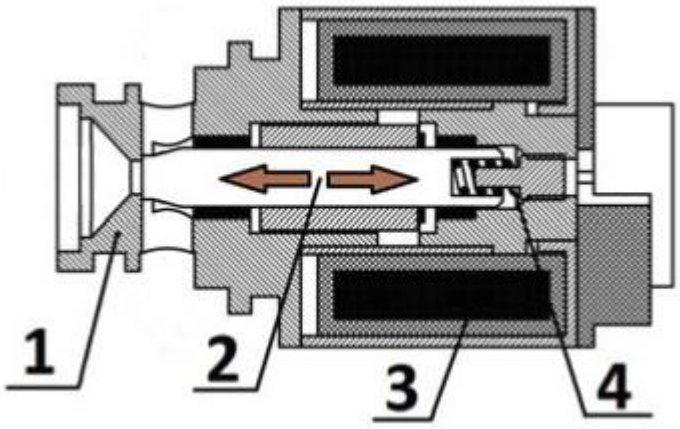

Figure 2-1: Schematic of a solenoid valve [Dül13]

2.2 Electromagnetism and material property of the solenoid

Valves are control elements in pneumatics, which convert pneumatic, electric or mechanical input variable into pneumatic output variable (pressure or flow rate), it constitutes the interface between the signal circuit and the power circuit of an installation. Because signal and data processing almost exclusively occurs electronically, rather high number of pneumatic valves actuated electromechanically.

A solenoid is an electromechanical device that used often in fluid power systems to actuate pneumatic or hydraulic valves; it converts electrical energy to kinetic energy. It is a long helical coil of wire through which a current running in order to create a magnetic field. The magnetic field created by a single strand of wire is weak. However, this magnetic field be strengthened by forming wire coils in a circular shape and by placing a magnetic core (iron or steel) through the wire coils to focus the magnetic field. Therefore, the magnetic field of the solenoid is the superposition of the fields due to the current through each coil. It is nearly uniform inside the solenoid and close to zero outside and is like the field of a bar magnet having a north pole at one end and a south pole at the other, depending upon the direction of current flow [Mur14] [Mur16].

It is known by the application of Ampere's Law, that a union of turns, when energized by electric current generate a magnetic field on its interior, being this field approximately parallel to the surface turns. Amperes law states in eq. 2-1 [Und1910] [Ton15], that the line integral of the magnetic field around a closed path (P), in defined length (L), is Proportional to the amount of permeability (μ), and the current (I_{enc}), that is enclosed by the path. This current is proportional to the number of turns (N) multiplied by the current (I) in each coil, so eq. 2-1 can be simplified to eq. 2-2 [Und1910] [Ton15]. Magnetic field produced when an electrical current flow through a simple conductor such as a length of wire or cable. Bending the wire into a circle and apply the right-hand grip rule to a single coil of the solenoid, the field lines still wrap around the current in the wire. In case of multi turns coil of solenoid the components of the field are concentrated in the interior of the coil and

is considerably weaker outside the coil. The longer the coil the weaker the field outside the coil will be as shown in Figure 2-2.

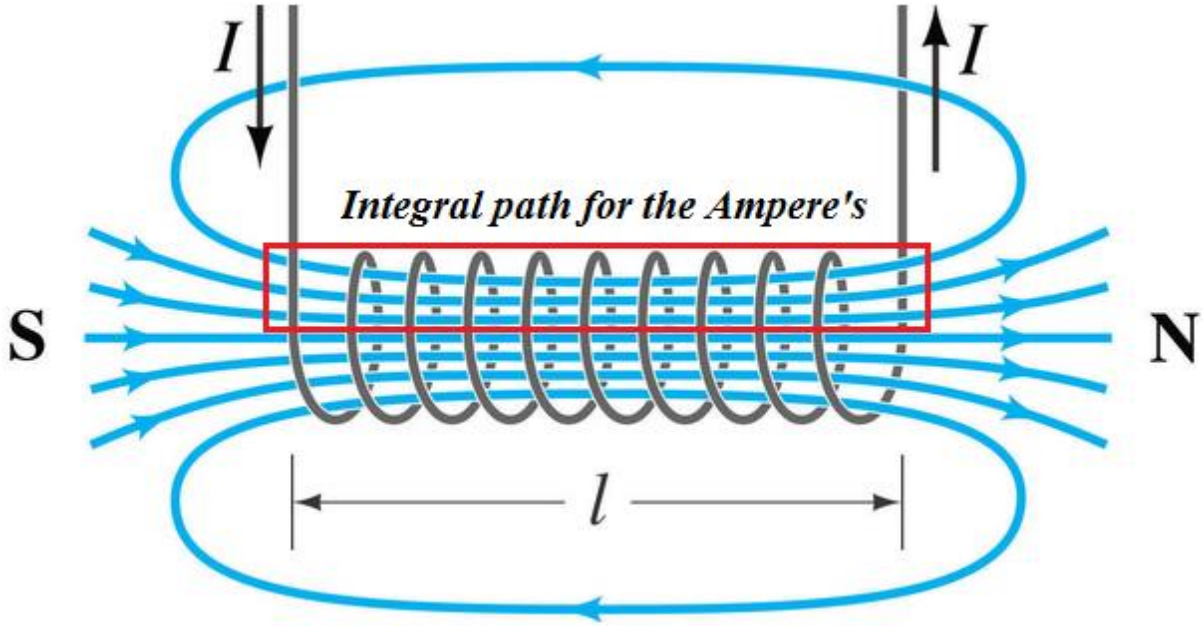

Figure 2-2: The concentration of Magnetic field inside and outside the solenoid [Wik18]

$$\oint_P \vec{B} \,.\, \overrightarrow{dl} = \mu . I_{enc} \qquad \text{eq. 2-1}$$

$$BL = \mu NI \qquad \text{eq. 2-2}$$

The lines which go to make up a magnetic field showing the direction and intensity are called Lines of Force-Magnetic Flux (Φ). But the number of lines of force within a given unit area is called the Magnetic Flux Density (B) is defined eq. 2-3 [Und1910] [Ton15]. The intensity of this field around the coil called Magnetic Field Strength-Magnetising Force symbol (H) is defined eq. 2-4 [Und1910] [Ton15], and it is proportional to the distance from it with the strongest point being next to the coil and progressively getting weaker further away from the coil [Und1910][Ton15].

$$B = \frac{\Phi}{A} \qquad \text{eq. 2-3}$$

$$H = \frac{I \times N}{l} \qquad \text{eq. 2-4}$$

Referring to the magnetic property of the solenoid, one of the most important characteristics is its saturation effect and it is easily understood by studying the magnetisation properties of the material (magnetic hysteresis) by which it firstly becomes magnetised and then de-magnetised. Saturation is the state reached when an increase in applied external magnetic field H cannot increase the magnetization of the material further, so the total magnetic flux density B more or less levels off. The relation between the magnetic field B and the magnetizing field H expressed as a function of magnetic permeability as shown in eq. 2-5 [Ele18].

$$\mathrm{B} = \mu.\mathrm{H} \text{ with } \mu = \mu_0.\mu_\mathrm{r}$$
$$\mu_0 = 4\pi \times 10 - 7\ \mathrm{H/m} \qquad \text{eq. 2-5}$$

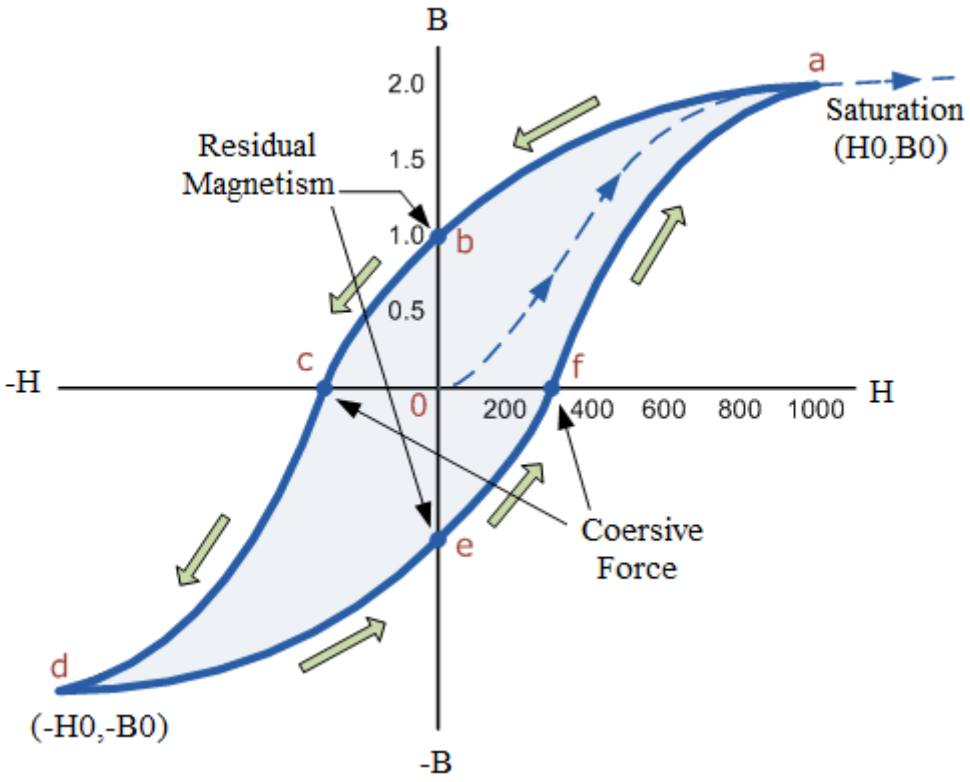

Figure 2-3: Magnetic Hysteresis Loop [Ele18].

Figure 2-3 shows the Magnetic Hysteresis loop behaviour of a ferromagnetic core graphically by plotting values of flux density (B) against the field strength (H) as the relationship between B and H is non-linear. The B-H curve follows the path of a-b-c-d-e-f-a as the magnetising current flowing through the coil alternates between a positive and negative value such as the cycle of an AC voltage [Ele18].

In magnetic designs, the core loss and the permeability are two essential parameters representing inherent characteristics of a magnetic material. Core loss is the loss that occurs in a magnetic core due to alternating magnetization, which is the sum of the hysteresis loss, the eddy current loss and the residual loss. Hysteresis loss caused by the magnetization and demagnetization of the core as current flows in the forward and reverse directions. This loss is proportional to the area encircled by the upper and the lower traces of the hysteresis loop. It is directly proportional to the frequency f and the peak flux density B^n as shown in eq. 2-6 [Tan95]. Eddy

current is inducing due to time-varying magnetic field, which applied to a specimen. These currents generate a certain amount of Ohmic loss, which is normally calling the eddy current loss. The mechanism for eddy current loss is the same as that in a conductor. Therefore, the eddy current loss is proportional to $f^2$and B^2 as shown in eq. 2-7 [Tan95]. The hysteresis loss and the eddy current loss account for large portion of the total core loss. The rest of it is normally calling the residual loss. Mechanisms behind these are complex. Experiences indicate that the residual loss is proportional to frequency f and peak flux density B as shown in eq. 2-8 [Tan95].

$$Pb = \eta \times Bmax^n \times f \times V \qquad \text{eq. 2-6}$$

$$Pe = Ke \times Bmax^2 \times f^2 \times t^2 \times V \qquad \text{eq. 2-7}$$

$$P_{fe} = Ke \times V \times B^n \times f^m \qquad \text{eq. 2-8}$$

2.3 Solenoid valves

A solenoid valve is an electromechanical device that uses the electric current to generate a magnetic field and thereby operate a mechanism which regulates the opening of fluid flow in a valve by controlling its plunger movement. Solenoid valves are the most frequently used control elements in fluids. Their tasks are to shut off, release, dose, distribute or mix fluids. They are found in many application areas. Solenoids offer fast and safe switching, high reliability, long service life, good medium compatibility of the materials used, low control power and compact design. It differs in the characteristics of the electric current they use, the mechanism they use to regulate the fluid, the strength of the magnetic field they generate, the type, and characteristics of fluid they control.

Solenoid valve are used in direct current DC or alternating current AC versions. DC solenoids produce magnetic fields with constant polarity, this magnetic field increases in intensity as the solenoid supply current increases in intensity, and it is typically use 12V or 24V, but also voltage until 220V is common. DC solenoids show less wear on the plunger or core tube, demonstrate a high holding force, robust winding, soft movement of the armature to avoid switching shocks, and does not fuse if the armature is stuck. On the other hand, the switching transistor of switching solenoid must be protected against voltage surges when it's in turning off mood, and so rectifier may be required. AC solenoid have an inductive resistance that varies according to the position of the armature, they are normally operated at 110V AC (50/60Hz) and 230V AC (50/60Hz). AC solenoid displays faster switching times, high force and it is possible to have direct connection to AC main. On the other hand, AC solenoid is sensitive against underload, have high heating in operation, its winding is sensitive and can fuse in case of overload, its armature must fully contact pole face after display and it necessary to do the measurement required to reduce vibration and eddy currents. So as a result, DC is more practical and is the most common version.

Solenoid valves can be designed in switching and proportional version. The switching solenoid valve have discrete behaviour; they are either ON or OFF, it is the preferred electro-mechanical converter in industrial pneumatics. Figure 2-4 show the structure of switching solenoid, the main components are the armature, the iron core and the excitation coil. The front surface of the armature and the iron core are polarized by turning on the excitation coil, this results in an attraction force which causes the armature to move to the right until it hits the iron core, as soon as electricity is shut off, the armature moves e.g. by spring force to its initial position. While the proportional solenoid is an advanced development of the switching solenoid, it adjusts the energy flow in a designed range due to an input signal to achieve the control function, the spool of proportional valves is progressively adjusted and needs to be positioned anywhere between the final positions, its force density is smaller than that in switching solenoid. The proportional solenoid in Figure 2-5 have this armature in pressure-sealed armature pipe which is screwed to the valve, the execution coil is moved over the armature pipe and therefore can be replaced without opening the liquid area [Hub14] [Hub16].

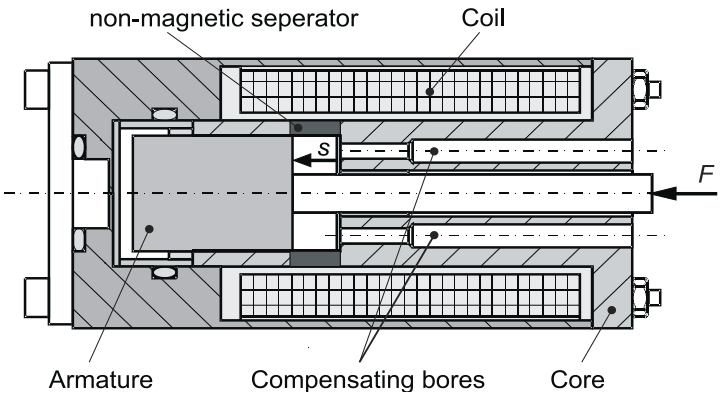

Figure 2-4 Structure of switching solenoid [Mur14].

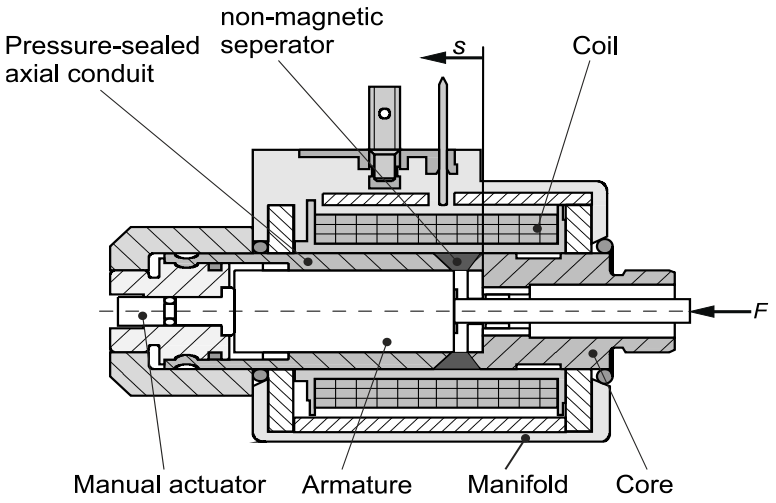

Figure 2-5 Structure of proportional solenoid [Mur14].

Figure 2-6 show the resulting solenoid force F for different electric current (i) in dependence on the armature stroke (s) for the switching and proportional solenoid. With the switching solenoid, the solenoid force increases as the armature stroke decrease, this based on the magnetic flux increase that results from the decrease in the gap between armature and iron core. While for the proportional one the solenoid force is independent of the stroke, and so large amount of the magnetic field are guided out radially from the armature without generating any axial force component. So, the maximum holding force with the same space is larger in switching solenoid than that in proportional one [Mur14] [Mur16].

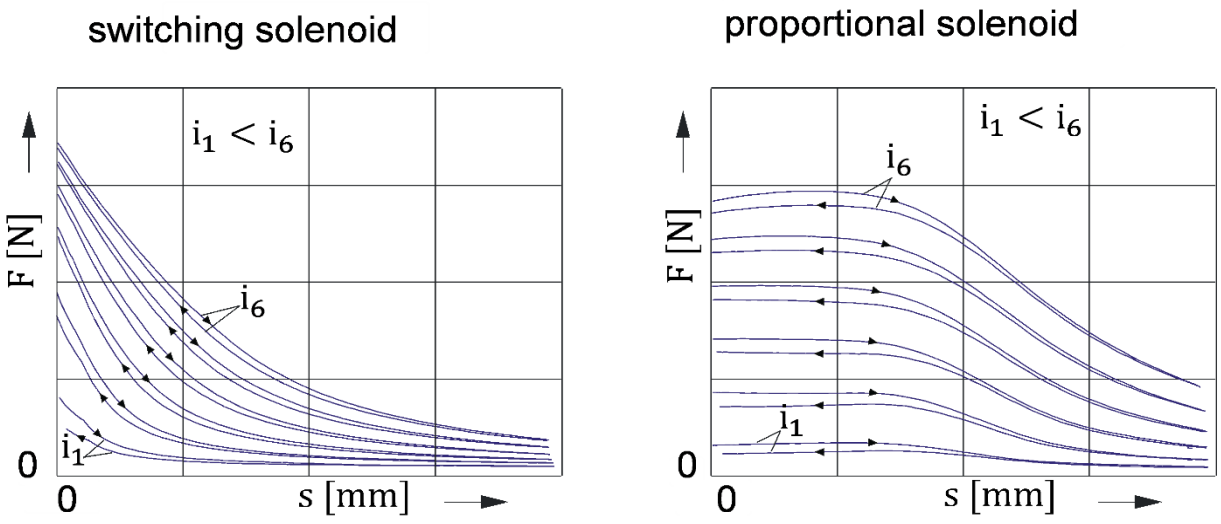

Figure 2-6: Solenoid force stroke characteristics (static) [Mur14].

2.3.1 Switching solenoid valve model 1

Solenoid system can be modelled using its own magnetic field closed circuit in which when a ferromagnetic material (plunger) is positioned at the coil axis edge, and there's electrical current through the coil, a magnetic field is concentrated in the interior of the material creating a magnetic force in the coil axis and pulling the plunger to the centre of the coil, so the created magnetic force is controlled by electrical injection. Based on that to model the solenoid plunger we must solve first its electrical and magnetic model, that rules the voltage in the coil's terminal and then the mechanical model that rules the force equation balance in the coil axis.

2.3.1.1 Electrical model

The electrical part of the switching solenoid valve can be modelled as an RL circuit as shown in Figure 2-7. In which the inductance L is not constant and is assumed to be a nonlinear function of the plunger position x and the input current i.

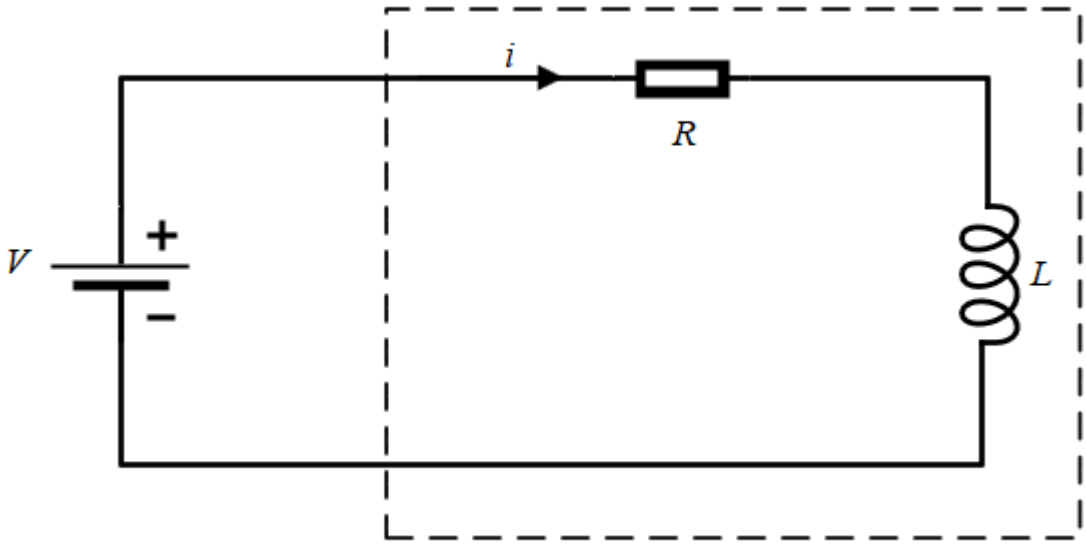

Figure 2-7: The equivalent circuit of solenoid valve [Ste08].

Using Kirchhoff's law, U is the equivalent voltage in the coil terminal and it's equal to the voltage from Lan's law plus the voltage from Ohm's law as shown in eq. 2-9 [Dem17].

$$U = \frac{\partial \lambda_{(x,i)}}{\partial t} + R.i_{(t)} \qquad \text{eq. 2-9}$$

As λ's depends on the two variables position of the plunger (x), current (i), and both are function of time, the derivative follows the chain's rule of the implicit derivative in eq. 2-10 [Dem17].

$$U = \frac{\partial \lambda_{(x,i)}}{\partial i_{(t)}}.\frac{\partial i_{(t)}}{\partial t} + \frac{\partial \lambda_{(x,i)}}{\partial x_{(t)}}.\frac{\partial x_{(t)}}{\partial t} + R.i_{(t)} \qquad \text{eq. 2-10}$$

But the solenoid valve flux linkage can be expressed as static inductive Ls(x,i) multiplied by the current i, as shown in eq. 2-11 [Dem17], and by substituting eq. 2-11 in eq. 2-10 we got the voltage balanced equation as a function of the inductance as shown in eq. 2-12 [Dem17].

$$\partial \lambda_{(x,i)} = \partial L_{(x,i)}.i(t) \qquad \text{eq. 2-11}$$

$$U = \left[\frac{\partial L_{(x,i)}}{\partial i_{(t)}}.i(t) + L_{(x,i)}\right]\frac{\partial i_{(t)}}{\partial t} + \frac{\partial L_{(x,i)}}{\partial x_{(t)}}.\frac{\partial x_{(t)}}{\partial t}.i(t) + R.i_{(t)} \qquad \text{eq. 2-12}$$

2.3.1.2 Magnetic Model

Due to the current in the coil, a magnetic field will appear inside the solenoid and result in a magnetic force affecting the armature. Regarding the electromechanical conversion, the attractive magnetic force on the plunger is the contribution of magnetic energy accumulated in the working air gap and core. Therefore, the electromagnetic force can be derived from the overall co-energy as shown in eq. 2-13 [Che93].

$$F_{mag} = \frac{\partial E_{(x,i)}}{\partial x_{(t)}} = \int_0^{i(t)} \frac{\partial \lambda_{(x,i)}}{\partial x_{(t)}} . di = \int_0^{i(t)} \frac{\partial L_{(x,i)}}{\partial x_{(t)}} . i(t)di \qquad \text{eq. 2-13}$$

2.3.1.3 Mechanical Model

As discussed in the previous section, the electromagnetic force F_{mag} affects the armature. However, other forces also have an influence on the armature which is: the spring force F_{hooke}, armature weight F_w, friction F_μ and viscosity force F_{vis}.Using Newton's Second Law yields, and together with assumed and provided information, the mechanical model for the valve can be derived as shown in eq. 2-14 [Dem17].

$$F_{tot} = -F_{mag} + F_{hooke} + F_w - F_\mu - F_{vis} \qquad \text{eq. 2-14}$$

In which

$$F_{tot} = M. \frac{\partial^2 x_{(t)}}{\partial^2 t} = M. \ddot{x} \qquad \text{eq. 2-15}$$

$$F_w = M. g. \cos\theta \qquad \text{eq. 2-16}$$

$$F_{vis} = \beta. \frac{\partial x_{(t)}}{\partial t} = \beta. \dot{x} \qquad \text{eq. 2-17}$$

$$F_{mag(x,i)} = \int_0^{i(t)} \frac{\partial L_{(x,i)}}{\partial x} . i(t)di \qquad \text{eq. 2-18}$$

$$F_{hooke} = -K. x_{(t)} \qquad \text{eq. 2-19}$$

$$F_\mu = M. g. \sin\theta . \mu_\mu \qquad \text{eq. 2-20}$$

$$k_4 = F_w - F_\mu \qquad \text{eq. 2-21}$$

Lastly, replacing all forces eq. 2-15 [Dem17] to eq. 2-21 [Dem17], the mechanical model of the solenoid valve become as shown in eq. 2-22 [Dem17]:

$$M.\frac{\partial^2_{x(t)}}{\partial^2 t} = -F_{mag(x,i)} - K.x_{(t)} + k_4 - \beta.\frac{\partial x_{(t)}}{\partial t} \qquad \text{eq. 2-22}$$

The objective from deriving the electrical, magnetic, and mechanical model is to study the equation exposed above for the magnetic circuit analysis and rewrite it in function of our output variables i(t) and x(t). But with the equations achieved it's unlikely that an algebraic solution will be found, and a numeric solution is needed. Then, the Differential Equations must be rearranged in a way that facilitates the construction of a flowchart in the Simulink Application, of the software Matlab as shown in eq. 2-23 [Dem17], eq. 2-24 [Dem17].

$$\frac{\partial i_{(t)}}{\partial t} = \left[U - \frac{\partial L_{(x,i)}}{\partial x_{(t)}}.\frac{\partial x_{(t)}}{\partial t}.i(t) - R.i_{(t)}\right].\left[\frac{1}{\left[\frac{\partial L_{(x,i)}}{\partial i_{(t)}}.i(t) + L_{(x,i)}\right]}\right] \qquad \text{eq. 2-23}$$

$$\frac{\partial^2_{x(t)}}{\partial^2 t} = \frac{1}{M}(-F_{mag} - K.x_{(t)} + k_4 - \beta.\frac{\partial x_{(t)}}{\partial t}) \qquad \text{eq. 2-24}$$

2.3.2 Switching Solenoid valve model 2

The second model is based on using the enhanced incremental energy method to determine the variation of the inductance as a function of the current and position. As in the previous model the coil model of solenoid valve can be equivalent to an R-L series circuit, and so we have the same dynamic equation for the electrical, magnetic and mechanical subsystem. Starting from eq. 2-12 we can obtain the dynamic inductance (L_d) as shown in equation eq. 2-25 [She13].

$$L_d = \frac{\partial Ls_{(x,i)}}{\partial i_{(t)}} . i(t) + L_{s(x,i)} \qquad \text{eq. 2-25}$$

This model is based on two assumptions to determine the dynamic and static inductance. At first, we assume that the solenoid valve is fixed in a certain location, then magnetic field energy Wm is shown in eq. 2-26 [She13].

$$W_m = \int e.\,idt = \int L_d\, idi \qquad \text{eq. 2-26}$$

When the current i_0 has disturbance Δi, the current currently is $i = i_0 + \Delta i$, and the variation of magnetic energy is shown in eq. 2-27 [She13].

$$\Delta W_m = Ld\frac{i^2 - i_0}{2} = Ld\frac{(\Delta i)^2 + 2i_0(\Delta i)}{2} \qquad \text{eq. 2-27}$$

As the current change, magnetic induction B and magnetic field strength H will change accordingly as shown below in eq. 2-28 [She13].

$$B = B_0 + \Delta B \quad , \quad H = H_0 + \Delta H \quad , \quad B = \mu . H \qquad \text{eq. 2-28}$$

According to the average magnetization curve of the material which is B –H the curve, the changes of the magnetic field energy are shown in eq. 2-29 [She13].

$$\Delta W_m = \iint HdBdV = \iint_0^{\Delta B} (H_0 + \frac{\Delta B}{\mu}) d(\Delta B) dV$$
$$= \int \left[H_0 \Delta B + \frac{(\Delta B)(\Delta H)}{2} \right] dV \qquad \text{eq. 2-29}$$

From the eq. 2-29 above, the nonlinear dynamic inductance (L_d) model of solenoid valve as shown in eq. 2-30 [She13].

$$L_d = \frac{\int (\Delta H)(\Delta B) dV}{(\Delta i)^2} \qquad \text{eq. 2-30}$$

Now according to the second assumption the iron core displacement is changes while current is constant, then the changes of the magnetic field energy are shown in eq. 2-31 [She3].

$$\Delta W_c = \iint HdBdV \qquad \text{eq. 2-31}$$

And the static inductance is shown in eq. 2-32 [She13],

$$Ls = \frac{\int B(\Delta H) dV}{i_0 (\Delta i)} \qquad \text{eq. 2-32}$$

Knowing that the iron core, valve body, shell and other magnetic component parts of solenoid valve use nonlinear magnetic material, so we need to determine the solenoid valve work area. Starting from the law of magnetic circuit which shown in eq. 2-33 [She13]:

$$NI = H_m l_m + H_g l_g \qquad \text{eq. 2-33}$$

When the air gap increases, magnetic flux surrounding the edges is serious proliferation, currently consider the flux edge diffusion phenomena. Eq. can be expressed as shown in eq. 2-34 [She13]:

$$NI = H_m l_m + \frac{B_r}{\mu_0} . (\frac{r}{r + l_g})^2 . l_g \qquad \text{eq. 2-34}$$

By B-H curve of the magnetic material and according to the solenoid valve operating current conditions, solenoid valves operating range can be determined within the scope of work values of (Br). Then take Br into eq. 2-34, we can obtain more data of Br on magnetic flux density, as a function of coil current I and displacement x as shown in eq. 2-35 [She13].

$$B_r = g(x, i) \qquad \text{eq. 2-35}$$

From eq. 2-35, eq. 2-30 and eq. 2-32, we can find the inductance model of static inductance and dynamic inductance, but to design this model the electromagnetic property is needed.

Finally, the solenoid valve model is designed based on model 1, and the missing data are presented using an experimental setup which will be explained in chapter 3.

2.4 Observers

The state of the inlet solenoid valve model can be written in the form of state space variables (SSV) equation, which is sometime not available or expensive to measure. To get an effective control and monitoring of the whole system, it is required at any time a reliable and accurate information about the SSV, to be able to apply state feedback control to the system, all its SSV must be available. Thus, to solve the problem of estimating system SSV, we need another dynamical system called the observer or estimator, connected to the system under consideration, whose role is to produce good estimate of the SSV of the original system [Gaj96].

The theory of observers started with the work of Luenberger (1964, 1966, 1971) [Lue64] [Lue66] [Lue71], so that observers are very often called Luenberger observers. State observer is a dynamic system whose purpose is to estimate the states based on available measurements or outputs of a dynamical system. It is not only useful in system monitoring, regulation and receiving the information of the internal variables of a system that are unknown, but also in detecting as well as identifying failures in dynamic systems, providing the basis of many practical applications. Since almost all observer designs are based on the mathematical model of the plant, the presence of disturbances, dynamic uncertainties, and nonlinearities pose great challenges in practical applications. Toward this end, to get the high-performance robust observer design, several advanced observer designs have been proposed. There are two main types for the observer the first one is linear observer and the second is nonlinear observer [Gaj96].

2.4.1 Linear Observer

According to Luenberger [Lue66], any system driven by the output of the given system can serve as an observer for that system, in which this observer has the same dimension as the original system. Consider a linear time invariant continuous time dynamic system in eq. 2-36, eq. 2-37.

$$\dot{x}(t) = Ax(t) + Bu(t)\ ,\ \ x(t_0) = x_0 = \text{unknown} \qquad \text{eq. 2-36}$$

$$y(t) = Cx(t) \qquad \text{eq. 2-37}$$

Where $x(t)$ is the system state vector $\in R^n$, $u(t)$ is the control input $\in R^m$, t is the time and y(t) is the output of the system $\in R^p$, with constant matrix A, B and C are the parameter of the state space model. Since the system output variables y(t) are always available, we may construct another artificial dynamic system of order (n) having the same matrices A, B and C as shown in eq. 2-38, eq. 2-39.

$$\dot{\hat{x}}(t) = A\hat{x}(t) + Bu(t) \quad ,\ \ \hat{x}(t) = \hat{x}_0(t) \qquad \text{eq. 2-38}$$

$$\hat{y}(t) = C\hat{x}(t) \qquad \text{eq. 2-39}$$

These two-output y and $\hat{y}$ are different as shown in eq. 2-40, since in the first case the system initial condition is unknown, and in the second case it has been chosen arbitrarily.

$$y(t) - \hat{y}(t) = \ Cx(t) - C\hat{x}(t) = Ce(t) \qquad \text{eq. 2-40}$$

$$e(t) = x(t) - \hat{x}(t) \qquad \text{eq. 2-41}$$

Where e(t) is the error signal eq. 2-41, that is generated from the output difference and it can be used as the feedback signal to the artificial system such that the estimation (observation) error e(t) is reduced as much as possible. This can be

physically realized by proposing the system-observer structure as given in the Figure 2-8.

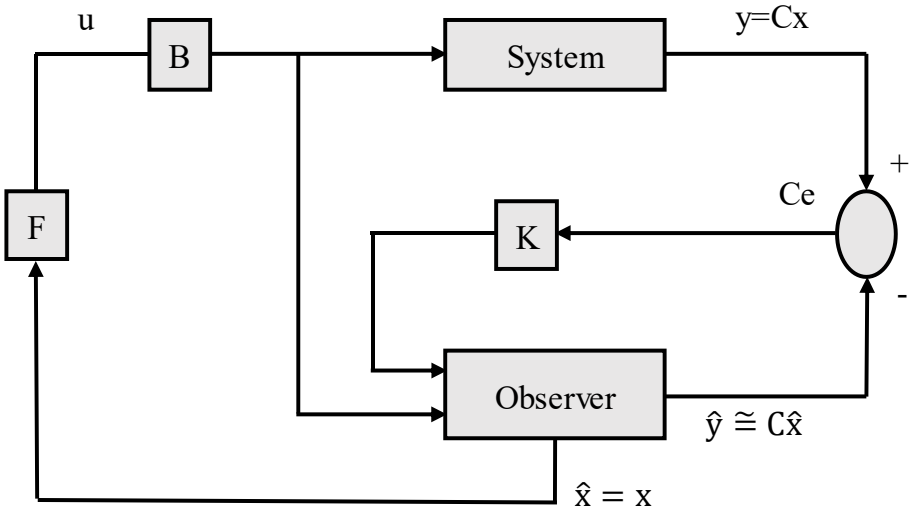

Figure 2-8: System Observer structure [Caj96].

In this structure (K) represents the observer gain and must be chosen such that the observation error is minimized. The observer alone is given by eq. 2-42.

$$\dot{\hat{x}}(t) = A\hat{x}(t) + Bu(t) + K\big(y(t) - \hat{y}(t)\big) \qquad \text{eq. 2-42}$$

By substituting eq. 2-39 in eq. 2-42, the observer input dynamic equation become as shown in eq. 2-43:

$$\dot{\hat{x}}(t) = (A - KC)\hat{x}(t) + Bu(t) + Ky(t) \qquad \text{eq. 2-43}$$

If we subtract the above two equations eq. 2-36 and eq. 2-43, this will give us the error dynamics of the observer as shown below in eq. 2-44:

$$\dot{e}(t) = \dot{x}(t) - \dot{\hat{x}}(t) = (A - KC)e(t) \qquad \text{eq. 2-44}$$

$$e(t) = e^{(A-KC)t}.e(0) \qquad \text{eq. 2-45}$$

The solution of this equation is an exponential function as shown in eq. 2-45, which means if this term (A-KC) is less than zero, then its good, since we know that our error will vanish over time and $\hat{x}$ will converge to x, but the significance of having a feedback loop around the observer is that we can control the decay rate of the error function by selecting the controller gain K accordingly. However, here the decay rate solely depends on the matrix A, and if there are some uncertainties in the mathematical model, this means you don't know the matrix A exactly. Therefor you can't control how quickly the error will vanish, the feedback gives more control over this equation and guarantees a faster elimination of the error, so faster estimated stats $\hat{x}$ will converge to true stats x. An optimal way of choosing the gain K is performed using Kalman filters [Caj96].

2.4.2 Nonlinear Observer: Sliding mode observer

The nonlinear system is said to be observable if it does not have any indistinguishable pair of states. This definition implies that a system can be observable, if there are no inputs which will render some states indistinguishable. This is because if any states are indistinguishable, they will be linearly dependent, and the observability subspace will be rank deficient. Since almost all observer designs are based on the mathematical model of the plant, the presence of disturbances, dynamic uncertainties, and nonlinearities pose great challenges in practical applications. Toward this end, the high-performance robust observer design problem has been topic of considerable interest recently, and several advanced observer designs have been proposed.

Sliding mode observer (SMO) belonging to the variable structure system (VSS) has proven to be an effective robust control strategy for incompletely modelled or nonlinear systems since its first appearance in the 1950s [Utk92] [Eme92]. One of the most distinguished properties of SMO is that it utilizes a discontinuous control action which switches between two distinctively different system structures such that a new type of system motion, called sliding mode, exists in a specified manifold. The peculiar characteristic of the motion in the manifold is its insensitivity to parameter variations, and its complete rejection of external disturbances [You96]. SMO has been developed as a new control design method for a wide spectrum of systems including nonlinear, time-varying, discrete, large-scale, infinite-dimensional, stochastic, and distributed systems [Hun93].

The design of SMO system is naturally carried out in two stages: -

1. The sliding surface is selected to achieve the desired sliding dynamics of the closed loop system.
2. The switching control law is selected to make the trajectory reach the sliding surface by pushing the system from any initial state towards sliding plane and ensures stable sliding mode.

The SMO problem is formulated for a general single input single output (SISO) nonlinear system is shown in eq. 2-46 and eq. 2-47 :

$$\dot{x} = a(x) + b(x)u \qquad \text{eq. 2-46}$$

$$y(t) = g(x) \qquad \text{eq. 2-47}$$

Where $x = [x_1, x_2, \dots, x_n] = [x, \dot{x}, \dots, x^{(n-1)}]$the system state vector, u is the scaler system input $\in R^m$, and the vector function a(x), b(x) $R^n \rightarrow R^n$ are continuously differentiable. The sliding function can be defined as linear combination of the system state and its order (for: s(x)-the sliding plane-sliding manifold) is usually the same as that of the Control input u, as shown in eq. 2-48, eq. 2-49:

$$s(x) \in R^m, s(x) = 0 \qquad \text{eq. 2-48}$$

And

$$s(x) = [s_1(x) \;\; s_2(x) \dots . s_m(x)]^T \qquad \text{eq. 2-49}$$

Then a Sliding mode control (SMC) $u(x) = [u_1(x)\; u_2(x) \dots u_m(x)]^T$may undergo discontinuities on some nonlinear surface $s_i(x) = 0$ in the state space and the SMC law for u(x) is evaluated based on the feedback values of sign(s(x)), in short it will be of the form shown below in eq. 2-50 [Utk09] and Figure 2-9 which state the main reasons why enforcing SMC is a promising method to control high-order nonlinear dynamic plants operating under uncertainty conditions.

$$u_i(t) = \begin{cases} u_i^+(x,t), & \text{where } s_i(x) > 0 \\ u_i^-(x,t), & \text{where } s_i(x) < 0 \end{cases} \quad i = 1, 2 \dots, m, \qquad \text{eq. 2-50}$$

Where $u_i^+(x,t)$ and $u_i^-(x,t)$ are continuous state functions, with $u_i^+(x,t) \neq u_i^-(x,t)$ and $s_i(x)'$s being continuous state functions.

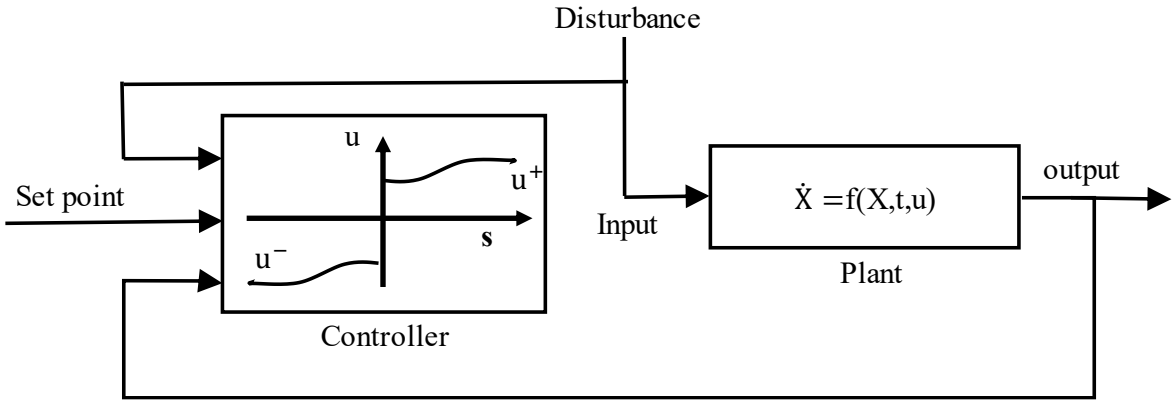

Figure 2-9: Systems with sliding mode control [Utk09].

The control action must move the system from any initial state $x_0 = x(t = 0)$ towards the sliding plane. This led to the so-called reachability condition, satisfied by means of proper controller design. The sliding plane is attractive if the following relation in eq. 2-51 [Kom12] is fulfilled:

$$s(x)\dot{s}(x) < 0, \forall\, s \neq 0 \qquad \text{eq. 2-51}$$

It can be noted that if the reachability is guaranteed globally the function shown below in eq. 2-52 [Kom12],

$$V = \frac{1}{2}s^2 > 0, \forall\, s \neq 0 \qquad \text{eq. 2-52}$$

Is the Lyapunov function for s, as eq. 2-53 [Kom12] is valid,

$$\dot{V} = \frac{1}{2}\frac{d}{dt}s^2 = s\dot{s} < 0, \forall\, s \neq 0 \qquad \text{eq. 2-53}$$

In order to ensure the finite time convergence, a stronger so called ‘’η-reachability’’ condition is used in eq. 2-54 [Kom12] and eq. 2-55 [Kom12].

$$\frac{1}{2}\frac{d}{dt}s^2 = s\dot{s} < -\eta|s|, \text{ with } \eta > 0,\ s \neq 0 \qquad \text{eq. 2-54}$$

$$\dot{s} \leq -\mathrm{Lsign}(s) \qquad \text{eq. 2-55}$$

Which can be satisfied with a discontinuous control with sufficiently gain of the form shown below in eq. 2-56 [Kom12],

$$u = -Lsign(s) \qquad \text{eq. 2-56}$$

Where sign(.) is the signum function defined by eq. 2-57 [Utk09],

$$sign(s) = \begin{cases} +1 \text{ if } s > 0 \\ 0 \text{ if } s = 0 \\ -1 \text{ if } s < 0 \end{cases} \qquad \text{eq. 2-57}$$

As we can see in the equation and figure above, enforcing sliding modes in system with discontinuous control enables order reduction, which results in decoupling and simplification of the design procedure. Furthermore, the element implementing discontinuous function u(x) has the input s(x) close to zero during sliding mode, where as its input takes finite values (the average values of the output). This means that the element implements a high gain, which is the conventional tool to suppress the influence of disturbance and uncertainties in the plant behaviour [Gao90] [Hun93] [Slo87] [Utk77] [Ray88].

For the considered system, applying eq. 2-56 [Kom12], we obtain

$$\dot{x} = a(x) + b(x).(-L.\,sign(s)) \qquad \text{eq. 2-58}$$

As the discontinuous system is applied the evolution of the system trajectory, in the phase plane consist of: finite time reaching phase (when the system is moved from the initial state towards the sliding manifold) and sliding face (when the system stats slides along the sliding plane to the origin). Because of the control discontinuity, investigation of the system dynamics in the sliding regime requires special method (Filippov control method, equivalent control method). In this approach for the determination of the system dynamic while remaining on the sliding surface the discontinuous control action is replaced by an equivalent continuous control signal (u_{eq}) , thus the system dynamic during the sliding mode is shown in eq. 2-59 [Kom12].

$$\dot{x} = a(x) + b(x)u_{eq} \qquad \text{eq. 2-59}$$

In which the equivalent control is as shown in eq. 2-60 [Kom12]:

$$u_{eq} = \frac{\nabla s(x)a(x)}{\nabla s(x)a(x)} = -\frac{L_a s(x)}{L_b s(x)}\,, L_b s(x) \neq 0 \qquad \text{eq. 2-60}$$

As the sliding mode is established by discontinuous control, one can assume that the information about the value of the equivalent control is comprised in the switching action, and the average value obtained by the low pass filtering of switching is as shown in eq. 2-61 [Kom12].

$$\tau \dot{u}_a + u_a = u_{eq} \qquad \text{eq. 2-61}$$

In which the filter time constant τ chosen small enough (the bandwidth of the filter covers all frequencies of the system and those of acting disturbance), and so it is close to the estimation of the equivalent control as shown in eq. 2-62 [Kom12].

$$u_a \approx u_{eq} \qquad \text{eq. 2-62}$$

2.5 The Bulge Test (valve application)

The Bulge Test is a new test design needed to supply material parameters at elevated temperatures (up to 950_C), and higher strain rate. It uses the gas as medium to account for the hot stamping conditions. For bulge testing at room temperature, a standard was already developed [DIN14]. The basic idea is to apply the membrane theory eq. 2-63 to calculate the not directly measurable stress at the bulge's pole (see ε in Figure 2-10 [DIN14]). The theory explains the relation between pressure P and stresses $\sigma_{1,2}$ along the principal-stress axis depending on the curvature radius $\rho_{1.2}$ and material thickness t_0. For a circular bulge, stress and curvature radius in both directions are equal [Mat17].

$$\frac{P}{t_c} = \frac{\sigma_1}{\rho_1} + \frac{\sigma_2}{\rho_2} \qquad \text{eq. 2-63}$$

The basic test setup according to this standard is shown in Figure 2-10. As depicted, the bulge test setup consists of a blank holder, a die, a sheet metal and a pressure supply. During the test cycle, first the sheet metal is fixed by the die and the blank holder and afterwards loaded with a fluid pressure from one side. As the pressure rises, the sheet metal starts to bulge through the die. By measuring the curvature radius and assuming continuity of the material, the material thickness at the centre t_c is derived and the stress calculated by. This testing method enables the characterization of material samples up to high strains. But material parameters don't only depend on the strain level ε. For example, strain rate $\dot{\varepsilon}$ and material temperature T are other important factors, which must be considered when dealing with material data. Thus, the strain levels and rates occurring during the test are only determined by material parameters and are not controlled. To address this issue, the HOT GAS BULGE TEST was developed, which allows to control the strain rate and level during the test. [Mat17].

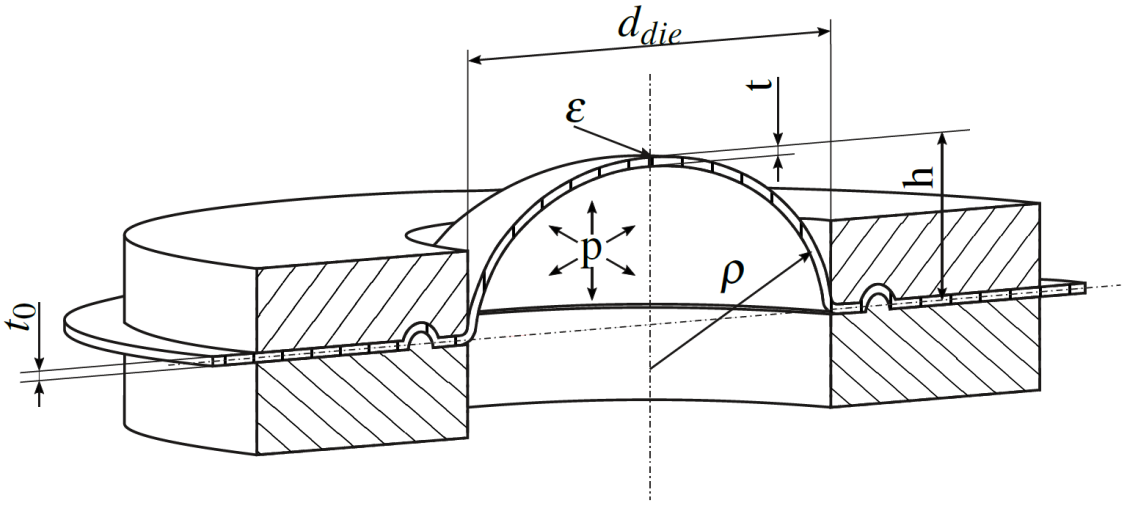

Figure 2-10: Scheme of a Bulge Test [DIN14].

Based on that, the pneumatic system used for the bulge test must be capable to vary the flow rate in a broad range precisely. Thus, a control algorithm was developed, that maps the required valves conductance into a valve combination to control the mass flow into the pressure chamber. In which the valve combination must be capable to vary the flow rate in a broad range precisely and therefore must possess comparably short response times.

There are only a few valves potentially suitable for the application were found. Fast proportional valves are necessary to achieve a controllability of the system. But no proportional valves acceptably fast and suitable for the pressure level were found. Thus, the decision is made to use switching valves. The valve combination is made of seven Era-Sib (EN52080) switching solenoid valves connected in parallel with a diameter of 0.7 mm as shown in Figure 2-11. All valves are connected in parallel to a gas bottle supplying the nitrogen. The bulge is located at the valves' outlet port. Piping is reduced to a minimum to bring down the dead volume. Pressure levels are measured at the source and inside the bulge. A laser tracking system measures the actual bulge height to derive the actual bulge volume. The full designed test bench is shown in

Figure 2-12.

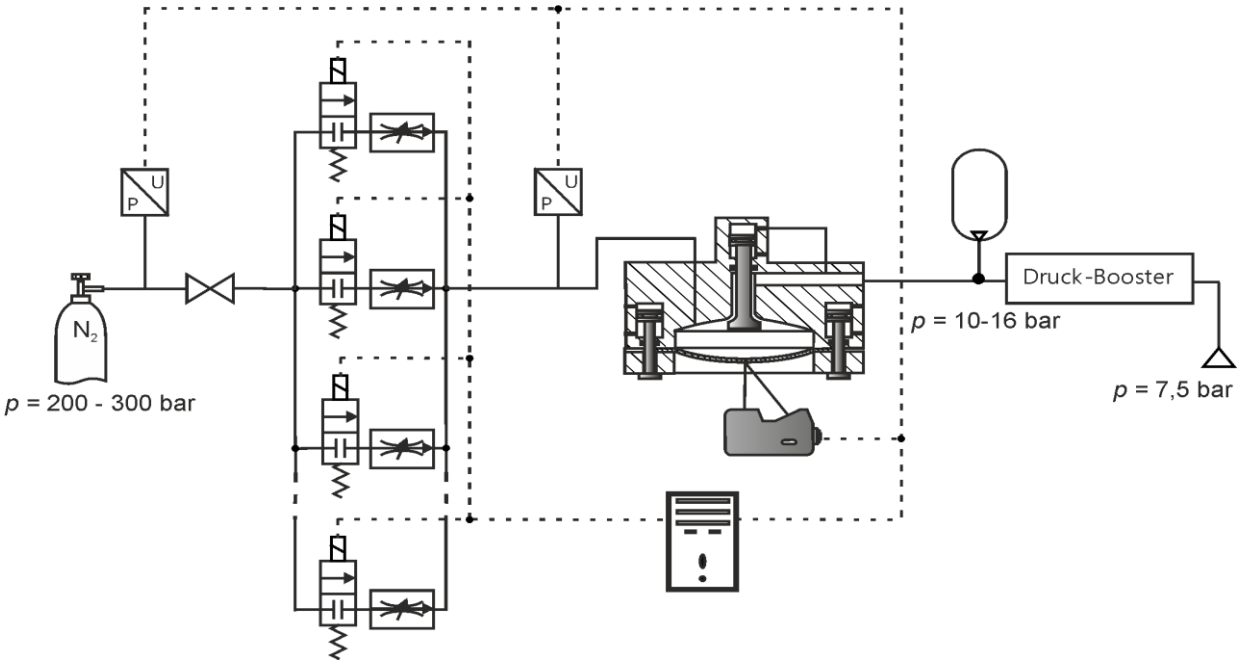

Figure 2-11: Circuit Diagram for the System [Mat14].

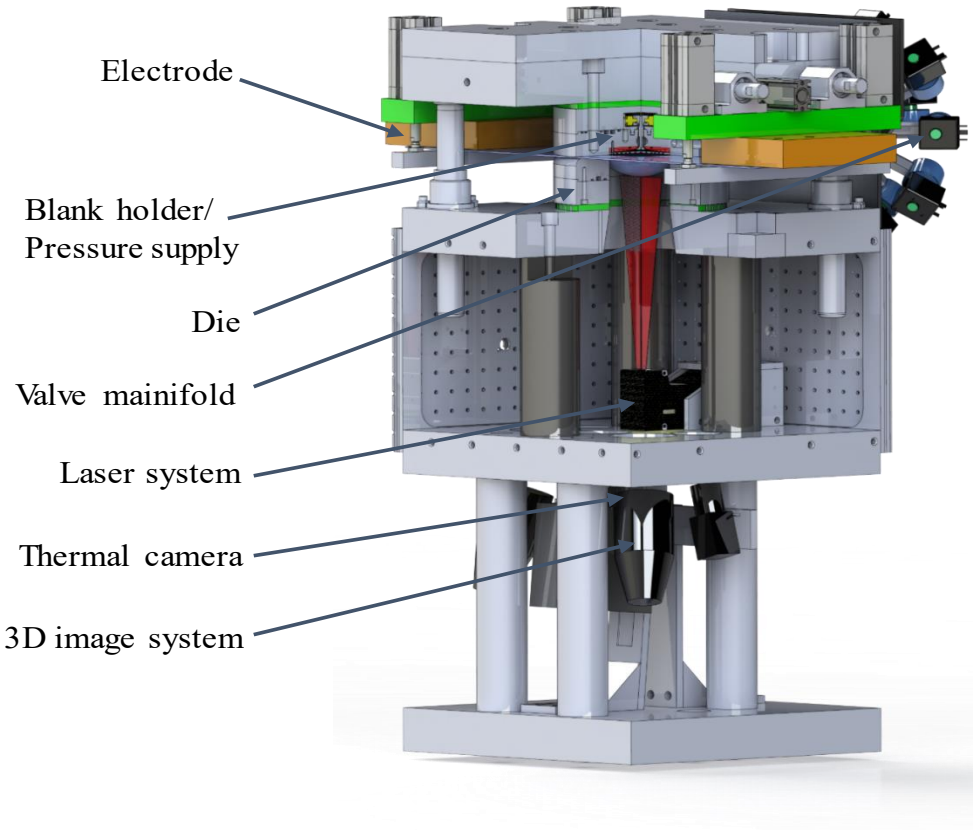

Figure 2-12: The test Bench [Bra16].

3 Experimental system of the valve measurement

This chapter presents the property of the used solenoid valve, and the experimental set up system which used to measure the missing parameter needed for the valve model.

3.1 EraSib En52080 Solenoid Valve

ERA-SIB is a French manufacturer, it offers the most complete solenoid valve ranges of high-quality direct acting and pressure assisted solenoid valves. EraSib En52080 2/2 NC Solenoid valve (two position, two ways direct operated) is shown in Figure 3-1, Figure 3-2. It is a modern valve that offers a fast operation, high reliability, long service life and compact design. It has a differential pressure range from 0 to 300 bar, a working temperature range of -10° to +50° C, and 20 milliseconds maximum opening-closing time. It can accommodate mediums with a temperature of up to 100°C. The valve is controlled by the electrical current that passes through the solenoid and it is initially closed, when the coil energized, magnetic field is created causing plunger to rise inside valve unsealing orifice, opining the valve and allows the pressurized gas to pass through the valve [Era19].

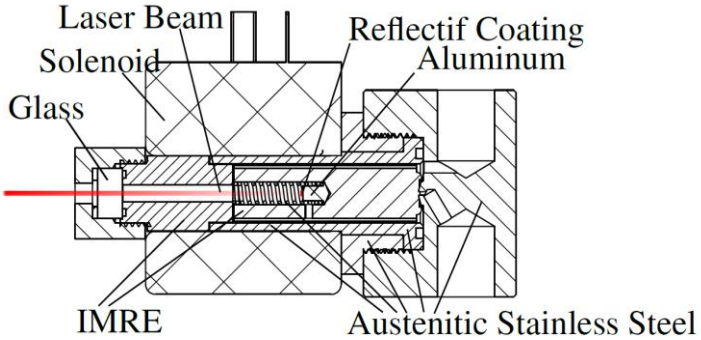

Figure 3-1: Cross section of the valve

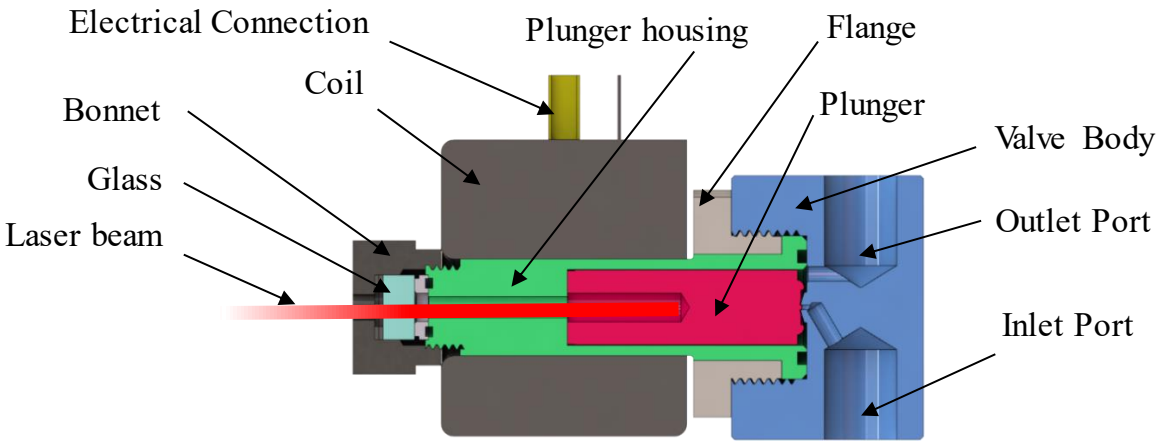

Figure 3-2: Simplified schematic of the Solenoid valve

3.2 Measuring and control system

The control system which used to build the solenoid model is based on its electrical, magnetic and mechanical model explained in part 2.3.1. For that goal the solenoid differential equation (eq. 2-23, eq. 2-24) are built in Matlab (see part 4.2). Because of lack of electromagnetic property of the solenoid valve material that is needed to measure the variation of electromagnetic force, inductance, derivative of inductance with respect to position, and with respect to current, as a function of the position (x) and the current (i). Consequently, another control system is designed to measure the electromagnetic force experimentally, and from it the inductance, the derivative of inductance with respect to position, and the derivative of inductance with respect to current, are derived as a function of position (x) and current (i).

Figure 3-3 shows the photo of the system which has been used to get the experimental data for the electromagnetic force of the solenoid valve. The system consists of PC, TB67H400A driver, the solenoid valve, force sensor, Amplifier, laser sensor, Polytec Vibrometer, LT1999 and INA111 amplifier, Beckhoff SPS and the 3D graph that represent the variation of electromagnetic force as a function of (x) position and (i) current. More explanation will be presented in part 4.1 about the electromagnetic force control system.

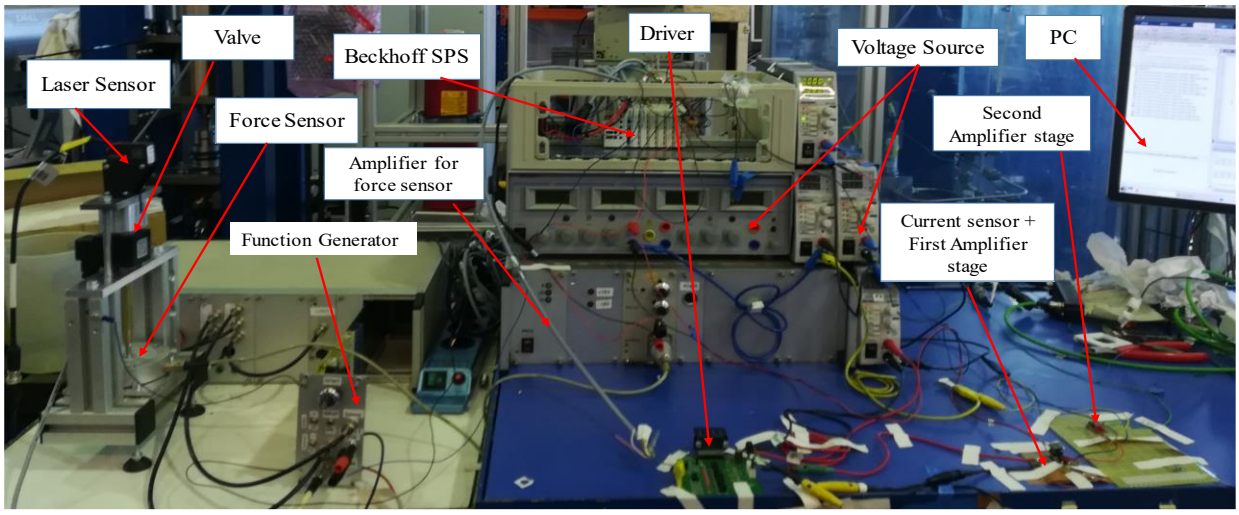

Figure 3-3: The electromagnetic force control system photo

4 Measuring the required parameters

This part presents a brief explanation for the control systems that are used to measure the required parameters which are the electromagnetic force, the inductance, the derivative of the inductance with respect to current, and the derivative of the inductance with respect to position. Then from them a look up tables is created and assigned to Matlab Simulink to substitute the above missing parameter in the solenoid valve model.

4.1 Measurement of the electromagnetic force

4.1.1 Test setup

The test setup used to measure the electromagnetic force is shown in figure Figure 4-1. The centre of the measuring chain is a Computer which generates reference signals logs and processes the measured data. The Computer is connected with the Beckhoff SPS which works as a D/A as well as an A/D converter and converts the reference signal to an Analog voltage V_{ref} which is sent to the TB67H400A driver. The created reference Voltage V_{ref} varies from 0V to 0.5V. The driver is used to set a constant output current I_{out} depending on V_{ref} as shown in eq. 4-1. It is connected to the solenoid valve, which is represented by its equivalent circuit (the inductor L1 and resistor R1=0.05 Ω in the blue box). In order to build a look up table this setup is used to measure three parameters. The current, the electromagnetic force of the solenoid as well as the plunger position.

To measure the electromagnetic force that is created by the solenoid, the force sensor (Tension and Comparison Load Cell - model 8523 and model 8531) is used. It is connected directly to the spool inside the valve, then the measured signal is amplified and sent to the Beckhoff SPS devise. In order to determine the current, the voltage across the known shunt resistor R1 is measured. This voltage is amplified using LT1999 instrument amplifier with a Gain (50). Due to high common mode voltages in the main loop the first amplifier stage LT1999 is separated by a

second amplifier stage IAN111 to insure the highest possible common mode rejection in order to reduce the disturbance in the measured signal. The voltage signal is send to the Beckhoff SPS device. To measure reliably and precisely the position x of the spool, we use Polytec Vibrometer, which is laser Doppler Vibrometer (LDV) to detect the variation of the position of the plunger inside the valve. It is a scientific instrument that is used to make non-contact incremental measurements. The laser beam from the LDV is directed at the plunger surface of the solenoid valve which is initially open. The output of an LDV is generally a continuous Analog signal with respect to zero position and is sent to Beckhoff SPS devise.

The Beckhoff SPS devise used to sample the received Analog signals with frequency (F= 50000 Hz), convert them to digital signal electromagnetic force, and send them to the computer. The computer processes the received data and create the look up table of the electromagnetic force as a function of the position and the current.

$$I_{out} = \frac{1}{5} \cdot \frac{V_{ref}}{R_{ss}} \quad , R_{ss} \cong 0.1\ \Omega \qquad \text{eq. 4-1}$$

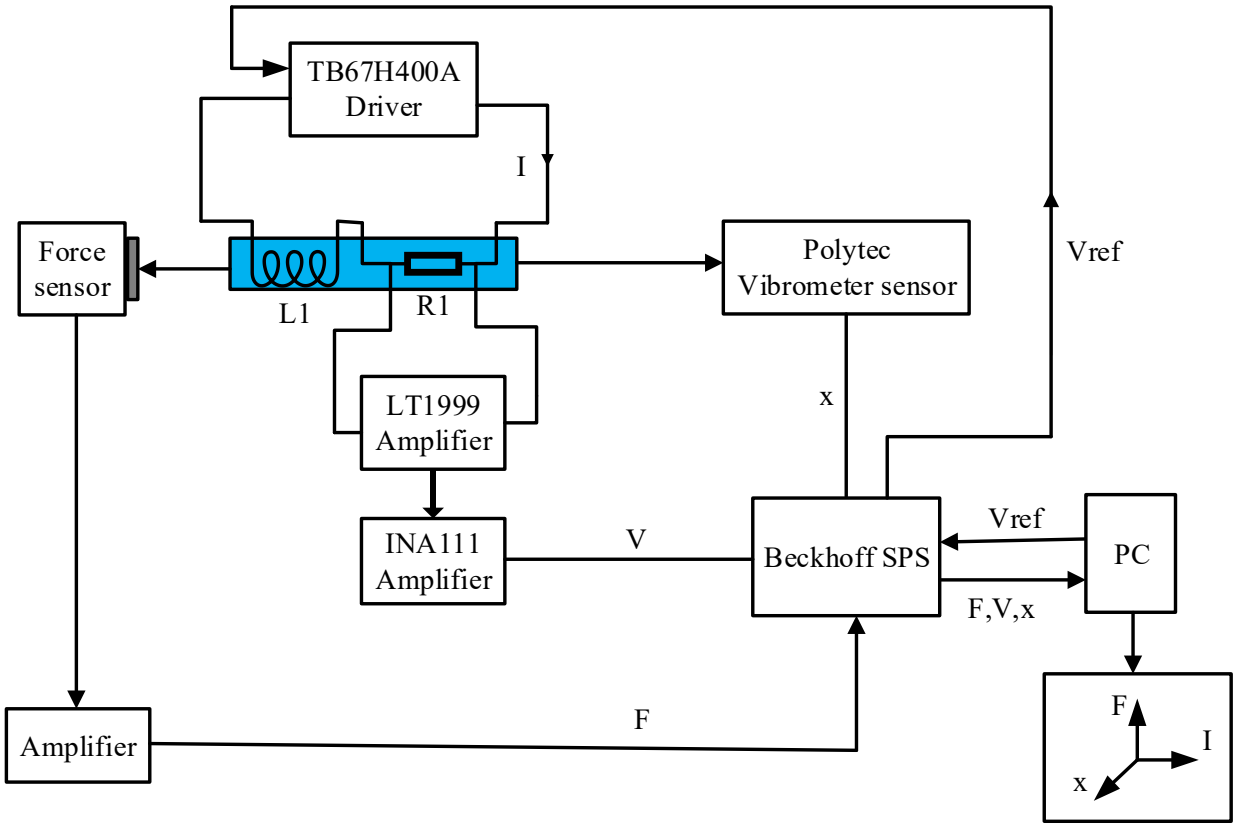

Figure 4-1: Simplified scheme of the electromagnetic force control system

4.1.2 Data processing / evaluation

The input current of our measurement test setup is ranged between Imin=0.1 and Imax=0.475A, and the input voltage is 36 V. As a first step, several measurements are done at different positions in the range of the air gab of the valve in which the current increases for each step every 2 seconds. As result of these measurements Beckhoff SPS device import to PC the data structures result of the test including 4 vectors:-the time, the position, the current, and the force. The second step would be rescaling the data so that the first measured value is at t = 0 for each vector. In the third step the measured data are plotted such that the incorrect measurements which resulted from the laser drifting is excluded out. In the fourth step, we make data smoothing to remove the noise and then the average mean of the measured value over each current level is taken. The fifth step would be visualizing the measurement data with Curve Fitting Toolbox, eliminating the outliers to exclude wrong measurement points and then export them to Matlab workspace. As a result of previous mentioned step, we got the electromagnetic force as a function of the position x and the current i. So the final step would be the integration and differentiation of the electromagnetic force $F_{mag(x,i)}$to calculate the inductance $L_{(x,i)}$, deriving the inductance with respect to position to get $\partial L_{(x,i)}/\partial x$, and deriving the inductance with respect to current to get $\partial L_{(x,i)}/\partial i$. The measurement results are shown in the Figures below.

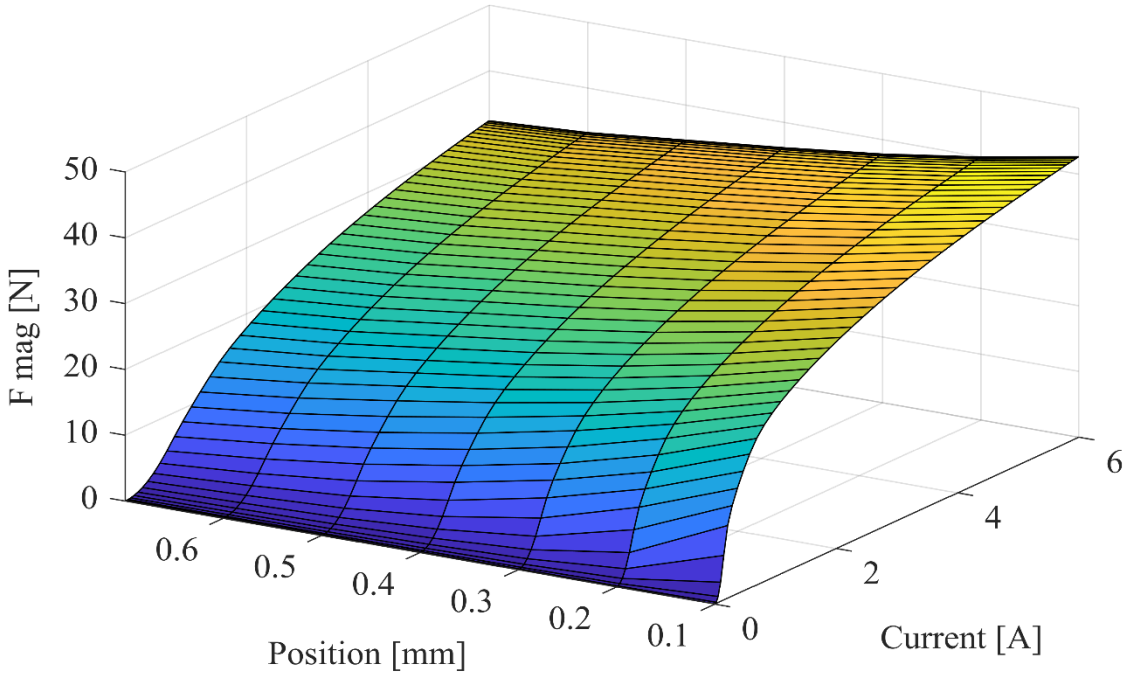

Figure 4-2: The electromagnetic force as a function of position and current

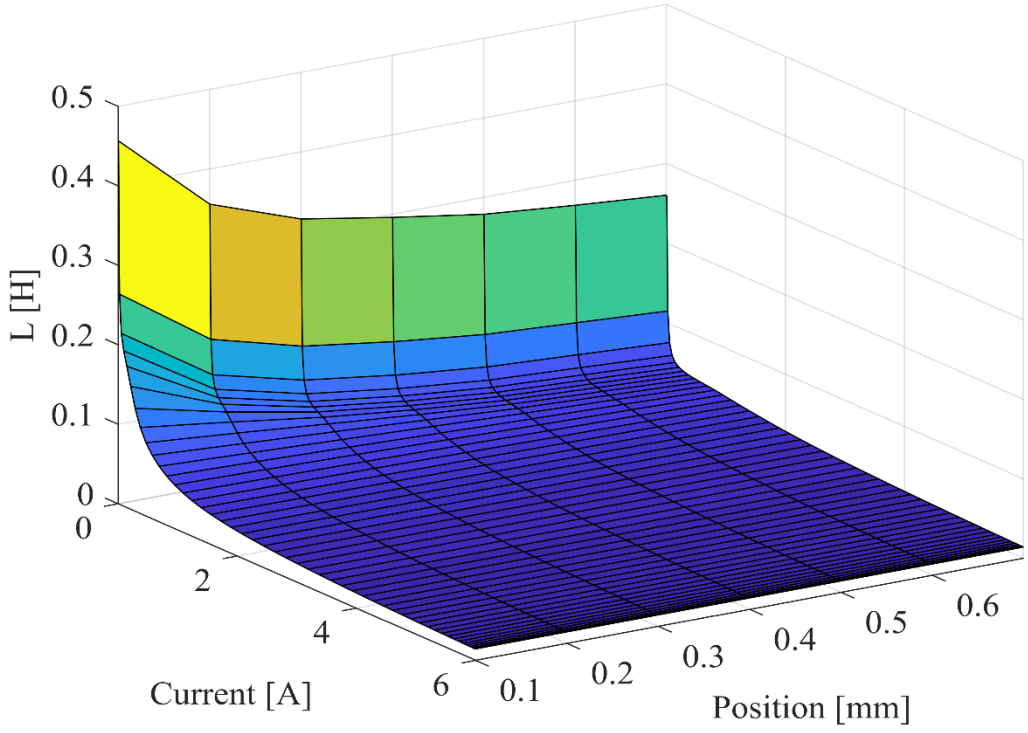

Figure 4-3: The inductance as a function of position and current

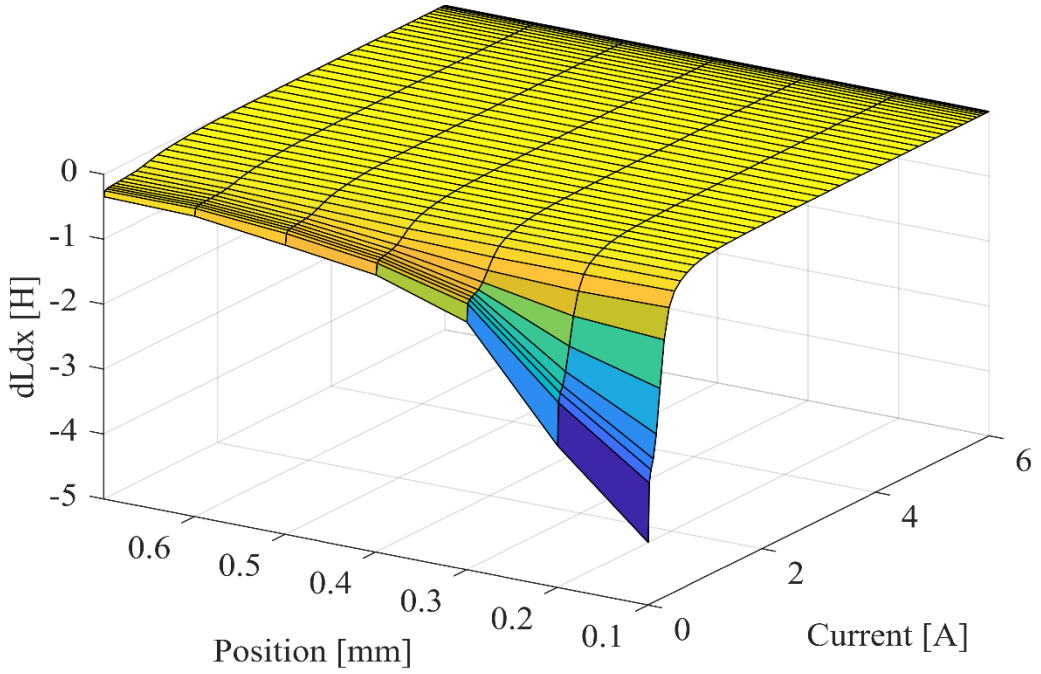

Figure 4-4: The derivative of the inductance with respect to position as a function of position and current

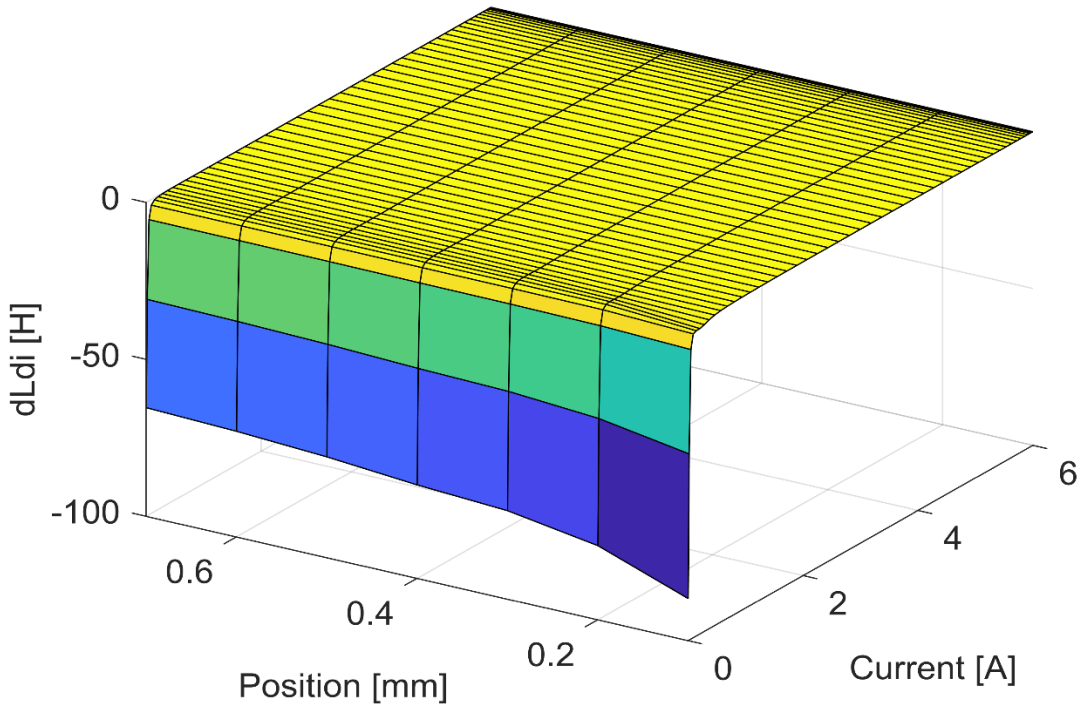

Figure 4-5: The derivative of the inductance with respect to current as a function of position and current

4.2 Simulation of valve model

The simulation of the solenoid valve system can be modelled using different models (see section 2.3.1 and 2.3.2). Because of lack of the electromagnetic property of the material of the valve, switching solenoid valve model 1 in section 2.3.1 is used. The objective of the model is to get the variation of the plunger position x (t) and the current i (t) with the time. By using the deferential equation (eq. 2-23 and eq. 2-24) which is derived from the electrical, mechanical, and magnetic equation of the solenoid valve, the valve design is constructed on Matlab as shown in 4.3.

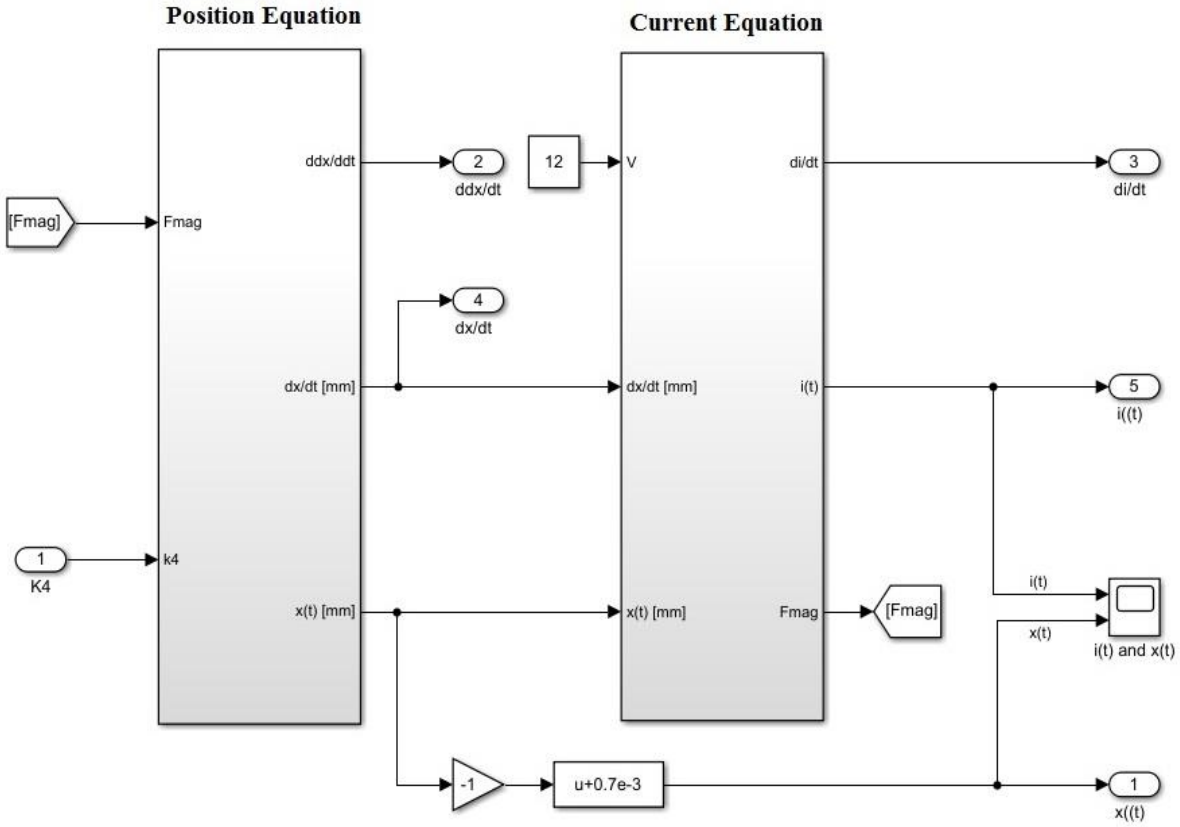

Figure 4-6: Superficial Visualization of Simulink design of the valve model

The entry position differential equation is designed based on eq. 2-24 as shown in Figure 4-7, and the entry current differential equation is designed based on eq. 2-23 as shown in Figure 4-8. The electromagnetic force, inductance, derivative of the inductance with respect to the position and with respect to current are represented as a look up table, such that as x and i are the inputs of the look up table. This look up table are obtained from the measured experimental data in section 4.1.2. The constants, weight, viscosity equation are represented in Matlab script file.

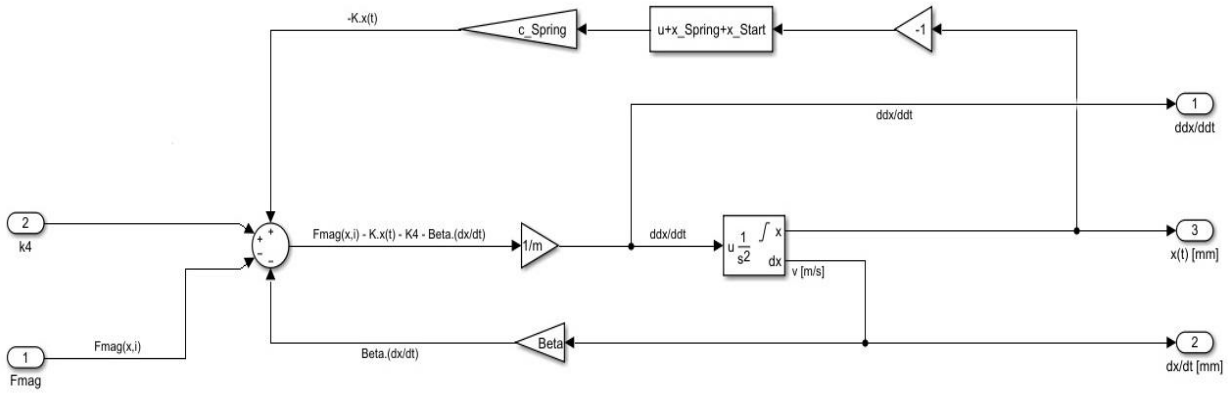

Figure 4-7: Position deferential equation design.

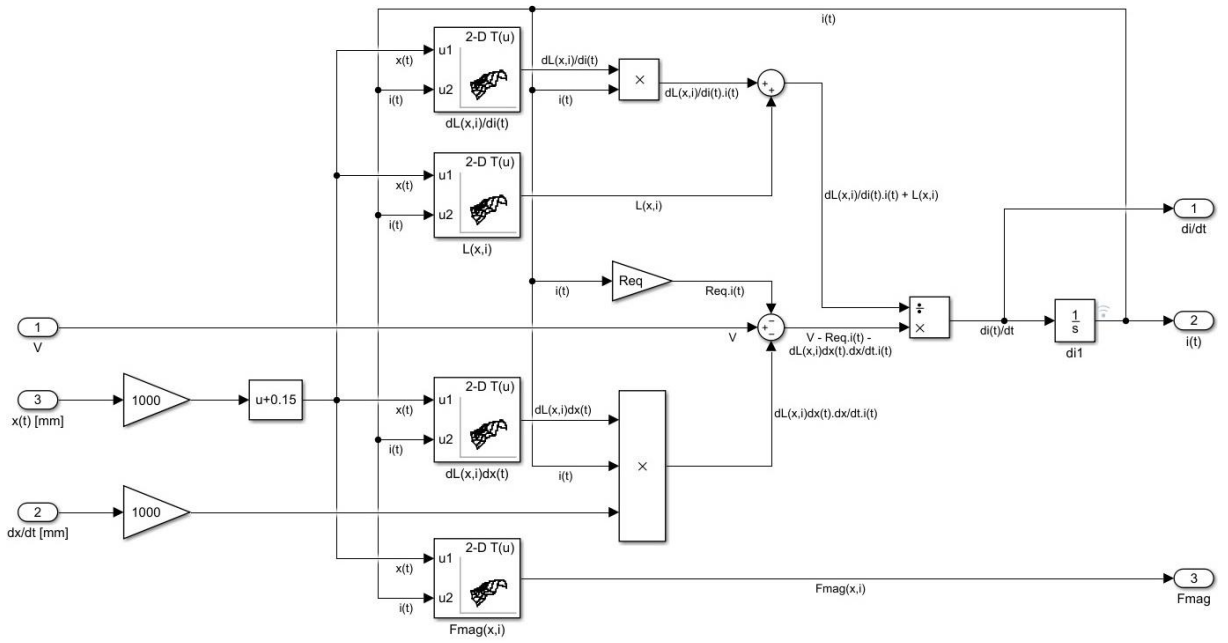

Figure 4-8: Current deferential equation design.

The simulation results of the outputs x (t) and current i (t) of the valve model are shown in Figure 4-9. The solenoid is operated by energizing the solenoid coil with an excitation voltage. Initially the valve is closed at 0.7 (mm), as soon as the solenoid is energized, the current increases, causing the electromagnetic force to increase until it becomes strong enough to move the plunger. At time 0.0073 seconds the plunger starts moving and the corresponding solenoid current is termed as I_{peak}. The plunger movement induces back EMF in the solenoid coil and this causes a brief reduction in the solenoid current. At time 0.0097 seconds, the plunger has moved completely and the current gets reduced to I_{valley}. After complete movement of the plunger, the solenoid current continues to rise until it reaches its maximum level limited by the coil DC resistance.

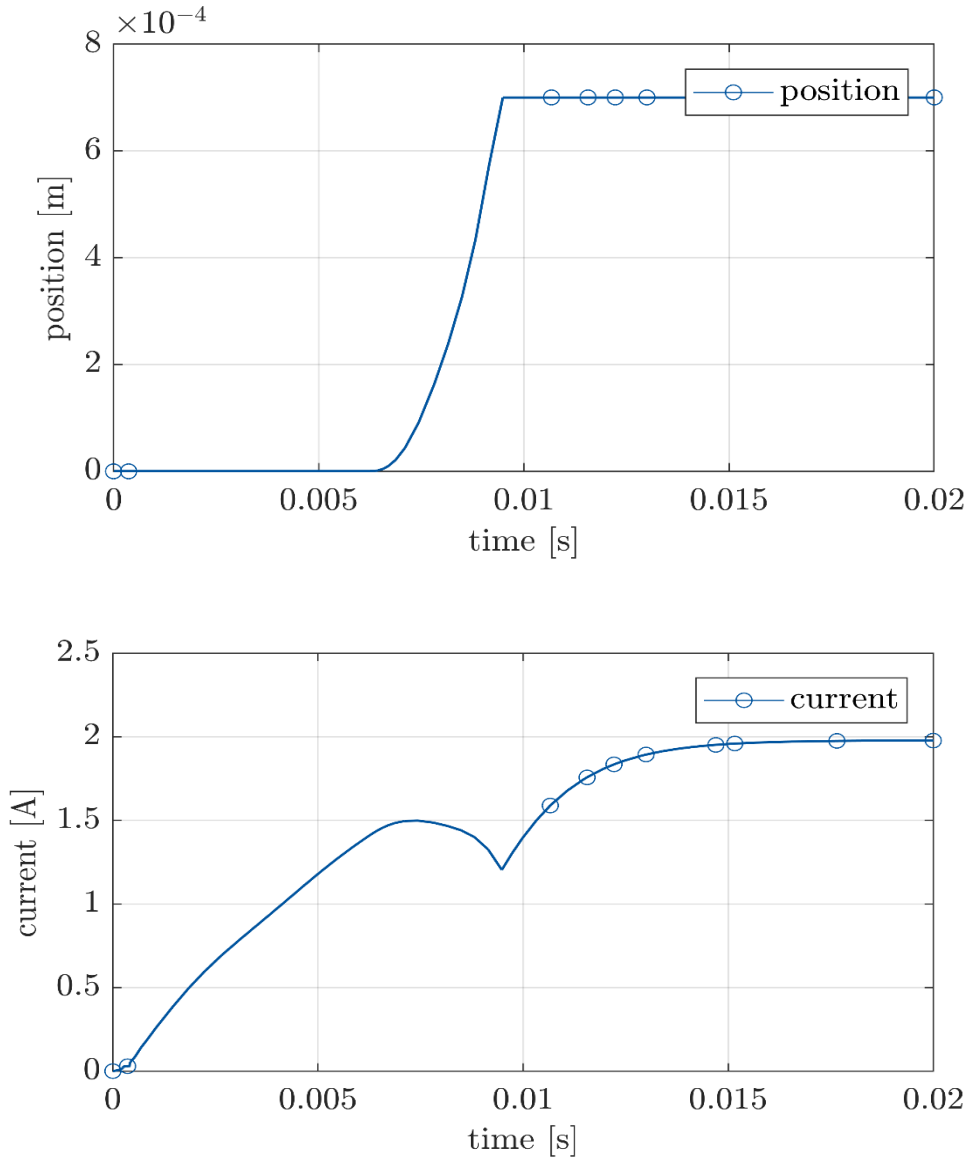

Figure 4-9: The simulation result of the valve model

5 Set up of the observer

As mentioned earlier in section 2.4.2, SMO is robust to disturbances and modelling error. So, a nonlinear SMO is designed to observe the plunger position under certain parameter uncertainties and bounded disturbance in this section. The inlet observer valve model can be designed based on first-order sliding mode algorithm in the form of state equation. The valve state of the most interest is the valve position which is obtained through double integration of the estimated plunger acceleration. This approach may lead to drifting (due to integration of biased noise and estimation errors), however, since the solenoid valves are switched between the fully open and completely closed positions the integration output maybe be limited and reset at the end stops and thereby circumvent long-term drifting effects.

5.1 SMO Model: - basic equations

The state estimation equations of the observer are based on the simplified dynamic system equations eq. 2-23 and eq. 2-24. Starting from previous mentioned equations, the inlet valve model can be written in the form of state equation as shown in eq. 5-1.

$$\begin{bmatrix} \dot{x}_1 \\ \dot{x}_2 \\ \dot{x}_3 \end{bmatrix} = \begin{bmatrix} \frac{U - A(x,i)\,.\,x_3\,.\,x_1 - R\,.\,x_1}{B(x,i)\,.\,x_1 + C(x,i)} \\ x_3 \\ \frac{1}{M}.\left(F_{mag(x,i)} - K\,.\,x_2 + k_4 - \beta\,.\,x_3\right) \end{bmatrix} \qquad \text{eq. 5-1}$$

$$y = [\,1\;0\;0\,]\,.x \qquad \text{eq. 5-2}$$

Where the state variable $x = [\,x_1, x_2, x_3]^T$ stands for $[\,i\,, x\,, \dot{x}]^T$ and

$$A(x,i) = \frac{\partial L_{(x,i)}}{\partial x_{(t)}}\;, \qquad B(x,i) = \frac{\partial L_{(x,i)}}{\partial i_{(t)}}\;, \qquad C(x,i) = L_{(x,i)} \qquad \text{eq. 5-3}$$

As shown in eq. 5-1 the current deferential equation is nonlinear, and the function of the electromagnetic force is not represented. For simplification, the current differential equation is linearized and considered as shown in eq. 5-4. The electromagnetic force is represented as polynomial function as shown in eq. 5-5, using the curve fitting method of the experimental data that are obtained in section 4.1.

$$\dot{x_1} = K_0 + K_1 \,.\, x_1 + K_2 \,.\, x_2 + K_3 \,.\, x_3 \qquad \text{eq. 5-4}$$

$$F_{mag(x,i)} = 14.65 - 20.83 * x_1 + 5.585 * x_2 \qquad \text{eq. 5-5}$$

The SMO has the following form in eq 5.6 [Tri14].

$$\dot{\hat{x}} = f(\hat{x}, \hat{\imath}) + \text{Lsign(e)} \qquad \text{eq. 5-6}$$

Where the estimation error is defined as $e = x - \hat{x}$. $sign(e)$ is the signal function.

$$\text{sign(e)} = \text{col}\,[\,\text{sign}(e_1), \text{sign}(e_2), \ldots, \text{sign}(e_n)] \qquad \text{eq. 5-7}$$

And

$$\text{sign(e)} = \begin{cases} +1, \text{if } e > 0 \\ 0, \text{if } e = 0 \\ -1, \text{if } e < 0 \end{cases} \qquad \text{eq. 5-8}$$

L is the SMO error compensation gain matrix, and

$$L = \text{diag}[L_1, L_2, \ldots, L_n] \qquad \text{eq. 5-9}$$

The boundary of gains is determined by Lyapunov stability theory, which will be discussed in the following part. Substituting the valve model shown in eq. 5-1 into the SMO eq. 5-6, the SMO of the inlet valve can be written as shown in eq. 5-10.

$$\begin{bmatrix} \dot{\widehat{x_1}} \\ \dot{\widehat{x_2}} \\ \dot{\widehat{x_3}} \end{bmatrix} = \begin{bmatrix} K_0 + K_1 \,.\, \widehat{x_1} + K_2 \,.\, \widehat{x_2} + K_3 \,.\, \widehat{x_3} + L_1 \text{sign}(e_1) \\ \widehat{x_3} + L_2 \text{sign}(e_2) \\ \frac{1}{M}.(14{,}65 - 20{,}83.\widehat{x_1} + 5{,}585.\widehat{x_2} - K\,.\,\widehat{x_2} + k_4 - \beta\,.\,\widehat{x_3}) + L_3 \text{sign}(e_3) \end{bmatrix} \qquad \text{eq. 5-10}$$

Where

$$e_1 = x_1 - \widehat{x_1} \quad , \qquad e_2 = x_2 - \widehat{x_2} \quad , \qquad e_3 = x_3 - \widehat{x_3} \qquad \text{eq. 5-11}$$

Assume that the observed coil current and spool position have enough accuracy and the difference between observed valve and real valve can be neglected. The assumption stands if the nonlinear SMO is stable and converges in finite time. With this assumption and eq. 5-8, the error system is derived as shown in eq. 5-12.

$$\begin{bmatrix} \dot{e_1} \\ \dot{e_2} \\ \dot{e_3} \end{bmatrix} = \begin{bmatrix} K_1 \,.\, e_1 + K_2 \,.\, e_2 + K_3 \,.\, e_3 - L_1 \text{sign}(e_1) \\ e_3 - L_2 \text{sign}(e_2) \\ \frac{1}{\text{M}} . (-20{,}83 . e_1 + 5{,}585 . e_2 - \text{K} \,.\, e_2 - \beta \,.\, e_3) - L_3 \text{sign}(e_3) \end{bmatrix} \qquad \text{eq. 5-12}$$

The error e_2 and e_3 cannot be calculated directly. For e_2, we just set the gain $L_2 = 0$, the system can still be stabilized. For e_3, the equivalent value method is used to determine the sign of e_3.

Consider the first equation of eq. 5-12 in sliding mode, where e_1, e_2 and $\dot{e_1}$ all equal to 0.

$$K_3 \,.\, e_3 = L_1 \text{sign}(e_1)$$
$$e_3 = \left\{ \frac{L_1 \text{sign}(e_1)}{K_3} \right\}_{eq} \qquad \text{eq. 5-13}$$

Where eq means the equivalent value of the contents inside the brackets. Then the SMO can be written as shown in eq. 5-14.

$$\begin{bmatrix} \dot{\widehat{x_1}} \\ \dot{\widehat{\text{x}_2}} \\ \dot{\widehat{\text{x}_3}} \end{bmatrix} = \begin{bmatrix} K_0 + K_1 \,.\, \widehat{x_1} + K_2 \,.\, \widehat{x_2} + K_3 \,.\, \widehat{x_3} + L_1 \text{sign}(e_1) \\ \widehat{\text{x}_3} \\ \frac{1}{\text{M}} . (14{,}65 - 20{,}83 . \widehat{x_1} + 5{,}585 . \widehat{x_2} - \text{K} \,.\, \widehat{\text{x}_2} + \text{k}_4 - \beta \,.\, \widehat{\text{x}_3}) + L_3 \text{sign}(\left\{ \frac{L_1 \text{sign}(e_1)}{K_3} \right\}_{eq}) \end{bmatrix} \qquad \text{eq. 5-14}$$

Error convergence of the SMO is proved by Lyapunov theory. The Chosen Lyapunov function is shown in eq. 5-15, and its time derivative is shown in eq. 5-16.

$$V = \frac{1}{2}.{e_1}^2 + \frac{1}{2}.{e_2}^2 + \frac{1}{2}.{e_3}^2 \quad \text{eq. 5-15}$$

$$\dot{V} = e_1\dot{e_1} + e_2\dot{e_2} + e_3\dot{e_3} \quad \text{eq. 5-16}$$

Substituting eq. 5-12 in eq. 5-16

$$\begin{aligned}\dot{V} = {} & K_1 . {e_1}^2 + K_2.e_2.e_1 + K_3.e_3.e_1 - L_1|e_1| + e_2.e_3 \\ & - \frac{20.85}{M}.e_1.e_3 + \frac{5.585}{M}.e_2.e_3 - \frac{K}{M}.e_2.e_3 - \frac{\beta}{M}.{e_3}^2 \\ & - L_3|e_3|\end{aligned} \quad \text{eq. 5-17}$$

We can have

$$\begin{aligned}\dot{V} \leq {} & K_1 . {e_1}^2 - \frac{\beta}{M}.{e_3}^2 \\ & + |e_1|.(K_2.|e_2|_{max} + K_3.|e_3|_{max} - L_1) \\ & + |e_3|.\left(-\frac{20.85}{M}.|e_1|_{max} + \left(\frac{5.585 - K}{M} - 1\right).|e_2|_{max} - L_3\right)\end{aligned} \quad \text{eq. 5-18}$$

Note that $K_1 < 0$ and $\beta > 0$ is always true condition, $L_1$and L_3 are chosen in way where the conditions in eq. 5-19 and eq. 5-20 are satisfied.

$$L_1 > (K_2.|e_2|_{max} + K_3.|e_3|_{max}) \quad \text{eq. 5-19}$$

$$L_3 > \left(-\frac{20.85}{M}.|e_1|_{max} + \left(\frac{5.585 - K}{M} - 1\right).|e_2|_{max}\right) \quad \text{eq. 5-20}$$

The Lyapunov function is negative semidefinite. According to the Lyapunov stability theory, the estimated state will converge to the real state, and the estimation error will approach zero in finite time.

Note that According to eq. 5-8, the nonlinear SMO loses observability when the coil current is constant with respect to time. But in this inlet-valve application, a PWM signal is used as the coil power so the coil current is chattering constantly, and the nonlinear SMO is always observable. By choosing bigger L_1 and L_3, the

nonlinear SMO is more robust to the modeling error. But overly large L_1 and L_3 will make observed states chatter around the real value.

5.2 SMO Model: - Structure

The SMO observer structure design is performed on Matlab Simulink using the estimated state equation (eq. 5-14). In which, the current output of the solenoid valve model is taken as an input for the error system of the observer, and the observer gain L1 and L3, the inputs K0, K1, K2 and K3 of the linearized current derential equation, are derived using optimization function. The observer structure is shown in Figure 5-1, Figure 5-2, and Figure 5-3.

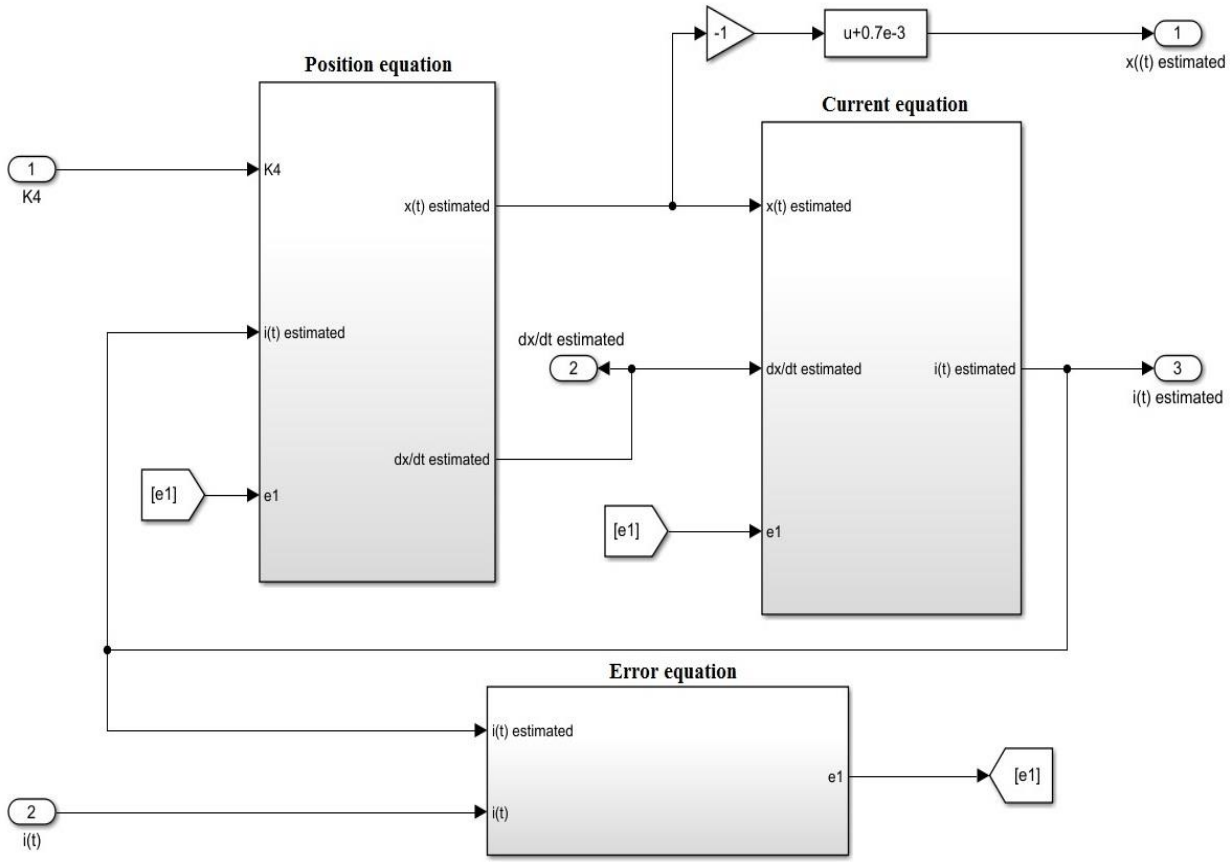

Figure 5-1: Superficial Visualization of Simulink design of the observer

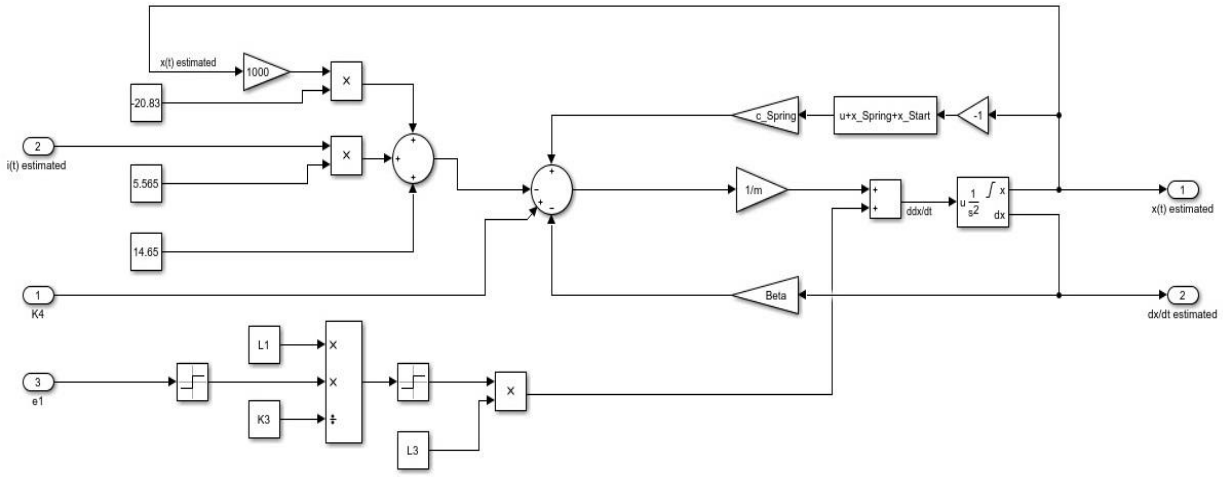

Figure 5-2: Position equation of the observer design.

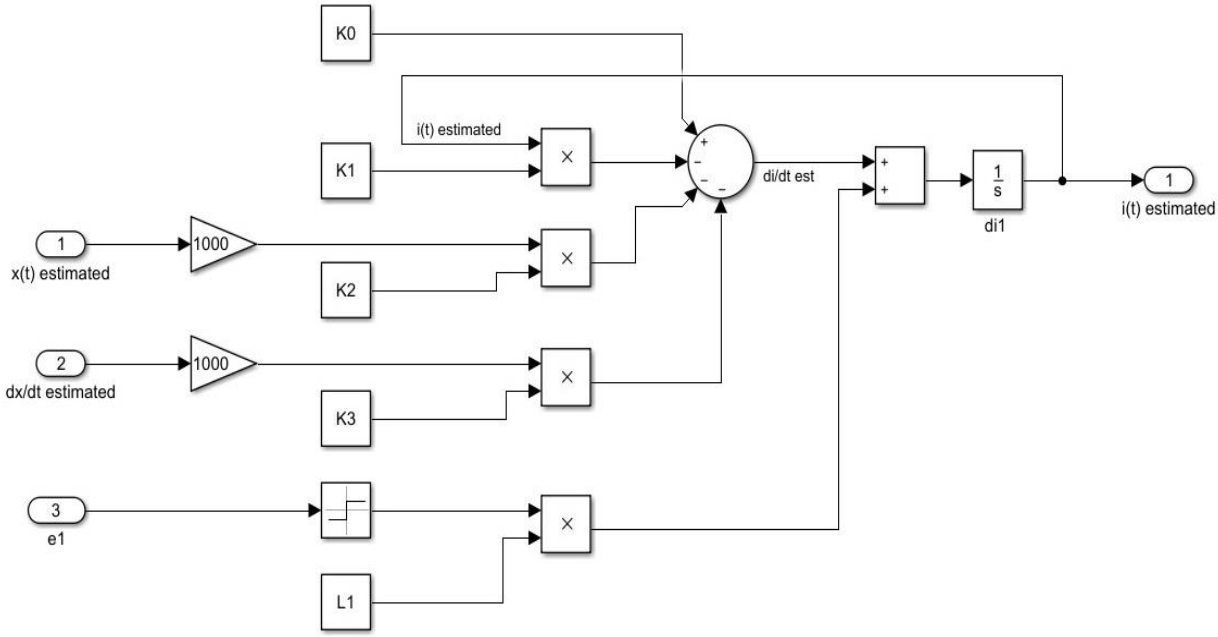

Figure 5-3: Current equation of the observer design.

5.3 SMO Model: - Parameter

As mentioned in section 5.2, the SMO parameter is assigned using optimization Matlab script function linked with Matlab Simulink block diagram. With Matlab Simulink diagram the absolute value of the integration of the estimated error equation e1 and e2 is balance in magnitude, added, and then the result is saved in workspace using simout block diagram as shown in Figure 5-4. At the same time the Matlab script optimization function is running to find the minimum error and the best fitting between the current and position function of the valve and the observer model using eq. 5-21. Based on the optimization result of the script function, the missing parameter is assigned to Matlab Simulink.

$$\text{f\_min} = \int |e|\, dt \qquad \text{eq. 5-21}$$

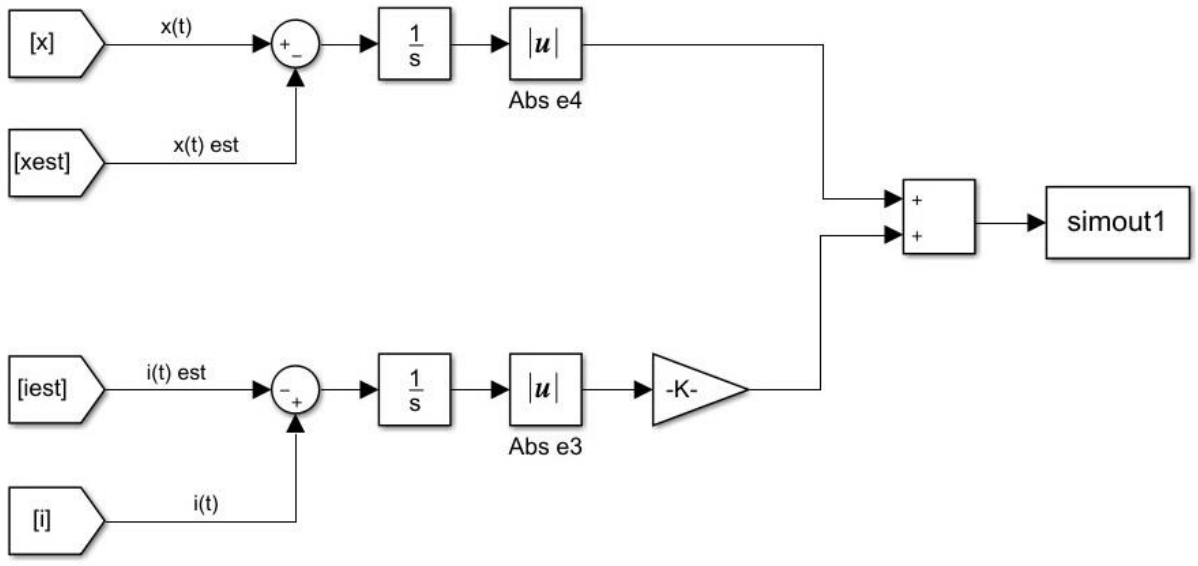

Figure 5-4: The estimation error block diagram

6 Validation of the observer's performance

The sliding mode observer is validated using Matlab Simulink. Starting from the parameter optimized result of the previous section, the SMO model is simulated. To find best fitting, the valve and the observer model is simulated several times and the parameter is tuned a little as shown in Table 6-1.

Missing parameter	Optimization result	After Tuning
L1	93.194	89
L3	-207.75	-206.989
K0	708.473	705.9
K1	-319.95	-305
K2	138.234	135.22
K3	1.0023	1.091

Table 6-1: The Required Parameter for the SMO Model

The simulation result for the valve and observer position, and current equation is shown in Figure 6-1 and Figure 6-2 respectively. The result didn't show totally fitting since the observer model is designed based on the linearized equation.

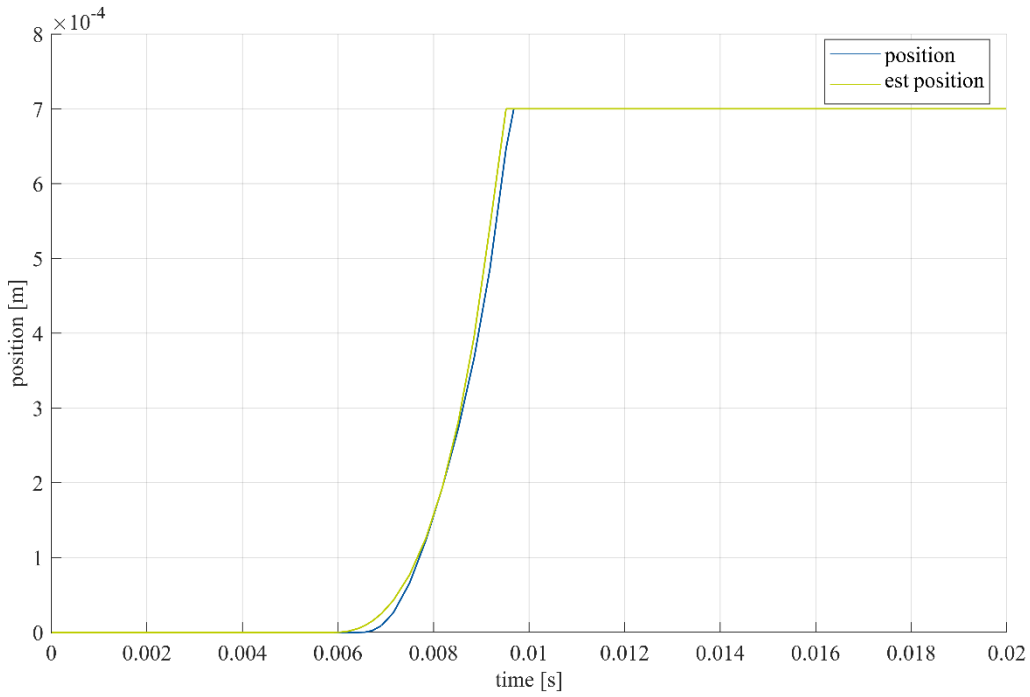

Figure 6-1: The Simulation result of the position equation of the valve and the observer model

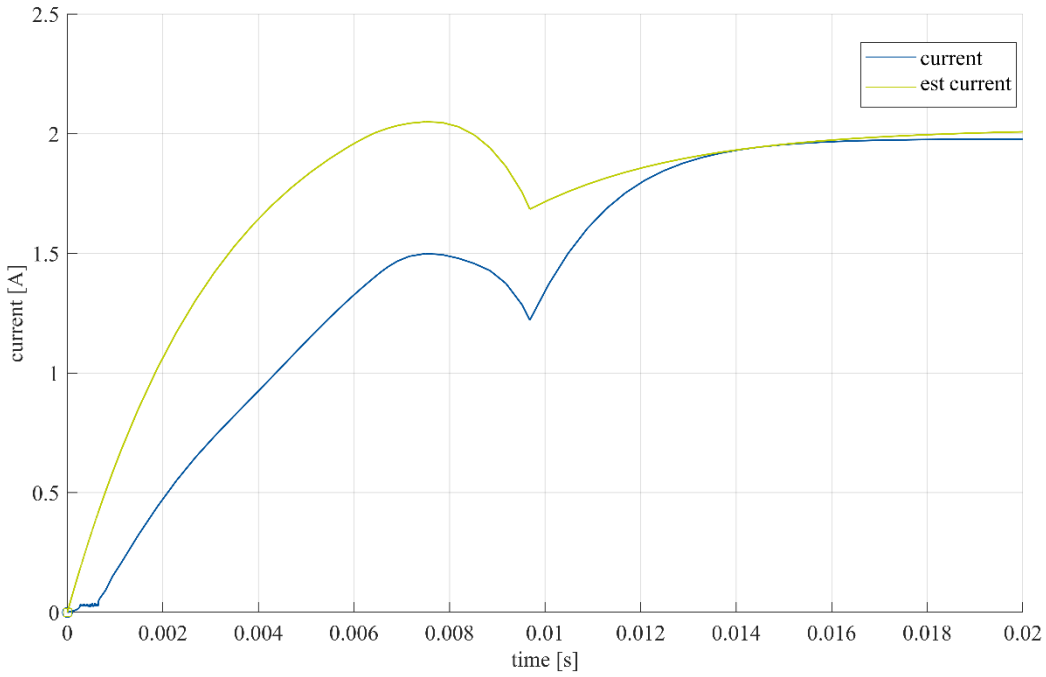

Figure 6-2: The Simulation result of the current equation of the valve and the observer model

7 Summary and outlook

In this thesis, an observer model for the switching Solenoid valve model was presented and validated. The observer based sliding mode theory was designed for this model. The sensorless estimation algorithm converged in closed loop. Though hysteresis and saturation where not modelled because of lack of the electromagnetic property of the material of the valve. The solenoid valve model is designed based on its deferential equation, and the missing parameter is modelled and validated experimentally. The observer based sensorless control strategy achieved almost exact regulation of the output, despite parametric uncertainties, hence it is robust. Plunger position and velocity were estimated from current measurements, and the estimates converged to their actual values asymptotically. A sliding mode based sensorless control strategy was implemented in simulation. Then the simulation result of the observer is compared with the valve model. Repeatability was acceptable and the actual position did not follow the desired trajectory exactly in every case due to noise.

For future work, the missing parameter K0, K1, K2, and K3 other linearization mothed could be used to find them and so we can got better optimization. Then using the sliding mode observer the designed model will be validated experimentally, by sitting up the observer model on the PC controller, and then compare the observer measurement with the laser system measurement in real time to cheek the accuracy of the model. The estimated plunger position result of the observer model will be used to control the mass flow rate resultant of the valve system, which needed in the bulge test.

The major contributions of this work could be stated as follows:-

- Design and simulate the solenoid valve model.
- Modelling, processing, and validating of the magnetic force of solenoidal valve to account for the effects of mutual inductance.

- Design and implementation of a nonlinear sensorless observer on the nonlinear dynamics of solenoidal valve, using the sliding mode methodology. It should be noted that there is no unique way of designing observers for nonlinear systems.

III Literature

/Dem17/	Arthur Demarchi, Leonardo Farconi, Adam Pinto, Rafael Lang, Roseli Romero, Ivan Silva	„ Modelling a Solenoid's Valve Movement “, Dissertation, Institute of Mathematics and Computer Science, University of Sao Paulo, 2017
/She13/	Cai Shengnian, Yang Man, Liang Yu	„ Sensorless Position Detection in Solenoid Valve Based on Inductance Model “, Dissertation, College of Information Engineering, Shenyang University of Chemical Technology Shenyang, China, 2013
/Che93/	Cheung, N., Lim, K., Rahman, M.	„Modelling a linear and limited travel solenoid “, industrial Electronics, Control, and Instrumentation, International Conference on, IEEE ,1993, S.1567-1572
/Und910/	Charles Reginald Underhall	„Solenoids Electromagnets and Electromagnetic Windings “, 2th ed., D. Van Nostrand Company, New York, 1910,
/Ton15/	David Tong	„Electromagnetism “, University of Cambridge Department of Applied Mathematics and Theoretical Physics, <http://www.damtp.cam.ac.uk/user/tong/em.html>, 2015, S.41-45
/Lue64/	David G. Luenberger	„Observing the state of a linear system”, IEEE Trans Military Electronics MIL-8, S.74–80, 1964
/Lue66/	David G. Luenberger	„Observers for multivariable systems”, IEEE Trans. Autom. Control, 11, S. 190-197, 1966.
/Lue71/	David G. Luenberger	„An introduction to observers”, IEEE Trans Automatic Control AC-16: S.596–602, 1971
/Ray88/	DeCarlo R. A., S. H. Zak, and G.P. Matthews	„ Variable Structure Control for Nonlinear Multivariable Systems: A Tutorial “, IEEE Trans. Aut. Contr., Vol. 76, NO. 3, pp. 212 232. 1988

/DIN14/	DIN Deutsches Institut fr Normung e. V.	„ Bestimmung der biaxialen Spannung/Dehnung-Kurve durch einen hydraulischen Tiefungsversuch mit optischen Messsystemen", 77.040.10, DIN EN ISO 16808:2014-11, Beuth Verlag GmbH, 10772 Berlin, 2014
/Bra16/	A. Braun, M. Waerder, G. Hirt	„FORMING LIMIT AND FLOW CURVE DETERMINATION OFHOT STAMPING STEELS USING A HOT-GAS-BULGE TEST", Proceedings of the 9th Forming Technology Forum 2016, Muenchen, Germany, pp. 5760, 2016.
/Ele18/	Electronics tutorials Team	„Electronics Tutorials Team ", <https://www.electronics-tutorials.ws/electromagnetism/magnetic-hysteresis.html>, visited on 22.12.2018
/Eme92/	S. V. Emelyanov	„ Variable Structure Control Systems ", Springer, Moscow: Nauka (in Russia), 1970
/Era19/	EraSib	„Erasib, made in France ", <http://www.erasib.com/erasib/media/Documents/Pdf/EN52080-EN52081_3.pdf?ext=.pdf >, visited on 3.11.2019
/Tan95/	F. Dong Tan, Jeff L. Vollin and Slobodan M. Cuk	„A Practical Approach for Magnetic Core-Loss Characterization ", Dissertation, IEEE Transactions on Power electronics, VOL. 10, NO. 2. MARCH 1995
/Gao90/	W. Gao	„ Fundamentals of Variable Structure Control Theory ", Beijing: Press of Science and Technology in China (in Chinese), 1990
/Mat17/	Gunnar Matthiesen, Hubertus Murrenhoff, Johannes Storz, Alexander Braun	„Pressure Control for A Hot Gas Bulge Test Using Parallel On-Off Valves", IFAS-IBF.RWTH Aachen University, Aachen, 2017

/Mur14/	*Hubertus Murrenjoff-Olivier Reinertz*	*„Fundamental of fluid power - Part 2: Pneumatics “, 2th ed., IFAS RWTH Aachen University, Aachen, 2014*
/Mur16/	*Hubertus Murrenjoff*	*„Fundamental of fluid power - Part 1: Hydraulics “, 8th ed., IFAS RWTH Aachen University, Aachen, 2016,*
/Hun93/	*J. Y. Hung, W. Gao, and J. C. Hung*	*„ Variable structure control: a survey “, Dissertation, IEEE Transactions on Industrial Electronics, Vol. 40, No. 1, S. 2–22, 1993*
/INC19/	*Solenoid Solutions INC*	*„Solenoid Solutions INC, made in France “, <https://www.solenoidsolutionsinc.com/infographics/how-a-2-way-normally-closed-solenoid-valve-works/>, visited on 3.11.2019*
/Dül13/	*Ivor Dülk, Tamás Kovácsházy*	*„A Sensorless Method for Detecting Spool Position in Solenoid Actuators “, Dissertation, Budapest University of Technology and Economics, 2013*
/Kom12/	*Jan Komsta, M. Sc., Bethlehem, PA*	*“Nonlinear robust control of electro-hydraulic system”, Dissertation, TU Darmstadt, S. 44–50, 2012*
/Slo87/	*J. J. E, Slotine and S. S. Sastry*	*„Tracking control of nonlinear system by sliding mode method “, International journal of control, vol.46, no. 3, pp. 1019- 1040, 1987*
/You96/	*K.D. Young,V. I.Utkin,*	*„ A control engineer’s guide to sliding mode control “, Dissertation, Proceedings of the IEEE International Workshop on Variable Structure Systems, S.1–14, Tokyo, Japan, 1996*
/NFP17/	*NFPA*	*„National Fluid Power Association“, <https://www.nfpa.com/home/AboutNFPA/What-is-Fluid-Power.htm>, visited on 20.12.2018*

/Ste02/	*Stefani, Shahian, Savant and Hostetter*	*„ Design of Feedback Systems “, Oxford University Press, New York, 2002, S.650–652*
/Tri14/	*Tristan Braun, Manuel Schwab, Florian Straußberger and Johannes Reuter*	*„State Estimation for Fast-Switching Solenoid Valves - A Nonlinear Sliding-Mode-Observer Approach”, Institute of System Dynamics, University of Applied Sciences Konstanz, Germany, 2014*
/Utk77/	*V. I. Utkin*	*„ variable structure system with sliding modes “, IEEE Transactions on Automatic control, vol. 22, pp. 212-222, 1977*
/Utk92/	*V. I. Utkin*	*„Sliding Modes in Control and Optimization “, Springer-Verlag, Berlin, 1992*
/Utk09/	*Vadim Utkin, Jürgen Guldner, Jingxin Shi*	*„Sliding Mode Control in Electro-Mechanical Systems “, 2nd ed., by Taylor & Francis Group, LLC, united states, 2009, S. 13-15*
/Ste08/	*Vidar Steinsland*	*„Modeling and Control of Retarder using ON/OF Solenoid Valves “, Dissertation, KTH electrical engineering Stockholm, S. 27, 2008*
/Wik18/	*wikimedia.org*	*„wikimedia.org “, <https://socratic.org/questions/if-current-passes-through-a-solenoid-will-two-consecutive-loops-move-towards-or->, visited on 20.12.2018*
/Gaj96/	*Z. Gajic and M. Lelic*	*„ Modern Control Systems Engineering “, Prentice Hall International, London, 1996, S. 435-477*

(H_0, B_0)

IV List of figures

V List of tables

VI Appendix

Matlab Code, initialization of the valve model and measurements.

```
% initialization script for valve model
%% Mechanical
x_Start=0.0007;                 %[m]
x_Limit=0.0007;                 %[m]
dx_dt_Start=0;                  %[m/s]
c_Spring=9000;                  %[N/m]
x_Spring=(13.4-12.25)*1e-3;     %[m]
%-----------
L0=0.0007;                      % constant
L1=101.1388;                    % constant
%-----------
 m= 0.0025;                     % [kg] - spool and pin
 g= 9.8  ;                      % [m/s]
 Teta= 0  ;                     % is one half of the cone angle of the seat
 Beta=  10;                     % the coefficent of viscosity force N.s/m
 N=   1900   ;                  % the number of turns of solenoid valve
 Req=  6.0645   ;               % the equivelent resistance in Ohm
 u =     0.2    ;               % friction coefficent neglected

 K4 = m*g*sin(Teta)+m*g*cos(Teta)*u; % friction coefficent neglected

 %% electrical

 load('Kennfeld_korrigiert');

 n_new      = 500;
 n_old      =   1000;
 x_new      =   x;

 i_new      =   n_old*i_average/n_new;

 L_new      =   (n_new/n_old)^2*L_average;

 %% Create new dLdi Look up table

 delta_i_m  =   0.5*(i_new(3:end)+i_new(1:end-2));

 delta_i    =   (i_new(3:end)-i_new(1:end-2));

```

```
40  delta_L_i  =  (L_new(:,3:end)-L_new(:,1:end-2));
41
42  dLdi_m     =  delta_L_i./repmat(delta_i,size(L_average,1),1);
43
44  dLdi_f = [ (L_new(:,2)-L_new(:,1))./(i_new(2)-i_new(1)),dLdi_m,...
45          (L_new(:,end)-L_new(:,end-1))./(i_new(end)-i_new(end-1))];
46
47  %% Create new dLdx_new Look up table
48  delta_x_m  =  0.5*(x_new(3:end)+x_new(1:end-2));
49
50  delta_x    =  (x_new(3:end)-x_new(1:end-2));
51
52  delta_L_x  =  (L_new(3:end,:)-L_new(1:end-2,:));
53
54  dLdx_m     =  delta_L_x./repmat(delta_x',1,size(delta_L_x,2));
55
56  dLdx_f = [ (L_new(2,:)-L_new(1,:))./(x_new(2)-x_new(1));dLdx_m;...
57          (L_new(end,:)-L_new(end-1,:))./(x_new(end)-x_new(end-1))];
```

Matlab Code, for current and position simulation result

```
1   %% for position simulation result
2   % data
3   X =current_sim.time;
4   Y =current_sim.data(:,1);
5
6    % legend text
7    legendtext='current';
8    % Axes Limits
9    xlim([0,.02]);
10   ylim([0,2.5]);
12
13   % Axes Labels
14   xlabel('time [s]');
15   ylabel('current [A]');
18
17    %% for position simulation result
19    % data
20    X =position_sim.time;
21    Y = position_sim.data(:,1);
22
23    % legend text
```

```
legendtext='position';
% Axes Limits
xlim([0,.02]);
ylim([0,8e-4]);

% Axes Labels
xlabel('time [s]');
ylabel('position [m]');
```

Matlab Code, the optimization Matlab script function to find the minimum error for the current and position function between the valve model and the observer model.

```
function optimizeL()

L_opt0 = [93 ,-207,707,-135,310,-1];

options=optimset('MaxIter',1000,'Display','iter','TolX',1e-3);

L_opt = fminsearch(@f_min,L_opt0,options);

end

function int_error = f_min(L)
% Set L1, L3, k5, k2, k3, and k4 in  Simulink

 L1 = L(1);
 L3 = L(2);
 k5 = L(3);
 k2 = L(4);
 k3 = L(5);
 k4 = L(6);
 set_param('valve_model/Subsystem2/Subsystem/Const4','Value',num2str(L3));
 set_param('valve_model/Subsystem2/Subsystem1/Const4','Value',num2str(L1));
 set_param('valve_model/Subsystem2/Subsystem1/Const','Value',num2str(k5));
 set_param('valve_model/Subsystem2/Subsystem1/Const2','Value',num2str(k2));
 set_param('valve_model/Subsystem2/Subsystem1/Const1','Value',num2str(k3));
 set_param('valve_model/Subsystem2/Subsystem1/Const3','Value',num2str(k4));

 sim('valve_model')
 int_error = simout.Data(end);
```

```
29    % return output
30
31    end
```